Searches for rare decays of the Higgs boson with CMS detector

Hao-Ren Jheng

on behalf of the CMS Collaboration

National Central University, Taiwan

Motivation

- Main decay channels/production modes of the Higgs boson have been discovered and measured → consistent with the SM within uncertainties

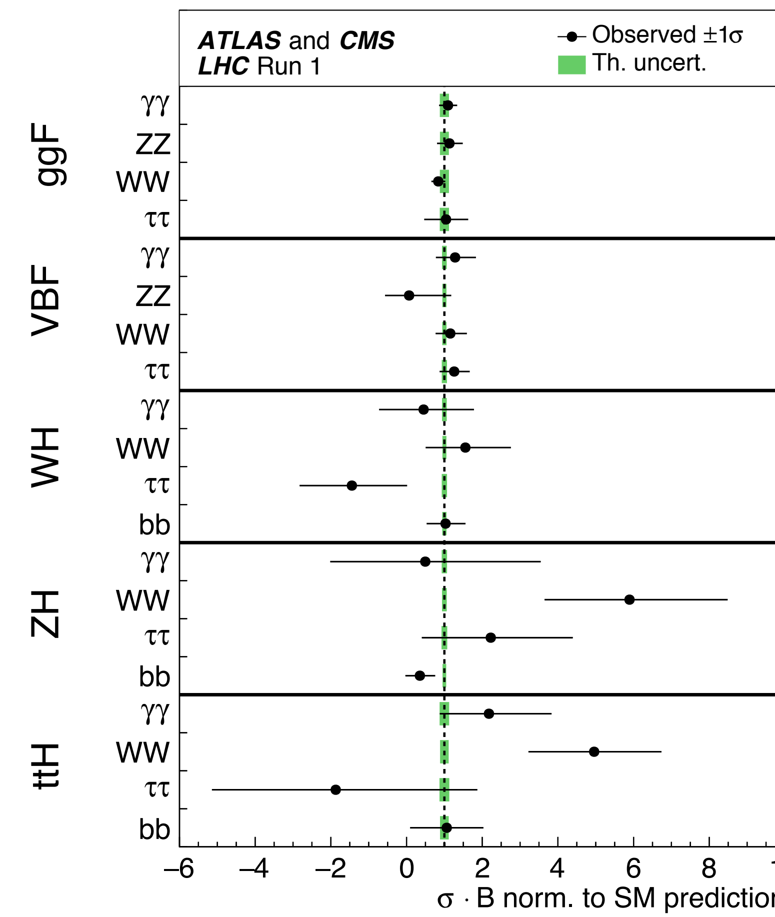

- The coupling measurements by both ATLAS and CMS (Run1 combination) indicate upper limit on B_{BSM}~O(30%)
  - Can non-SM couplings hide inside? Where it/they can be?

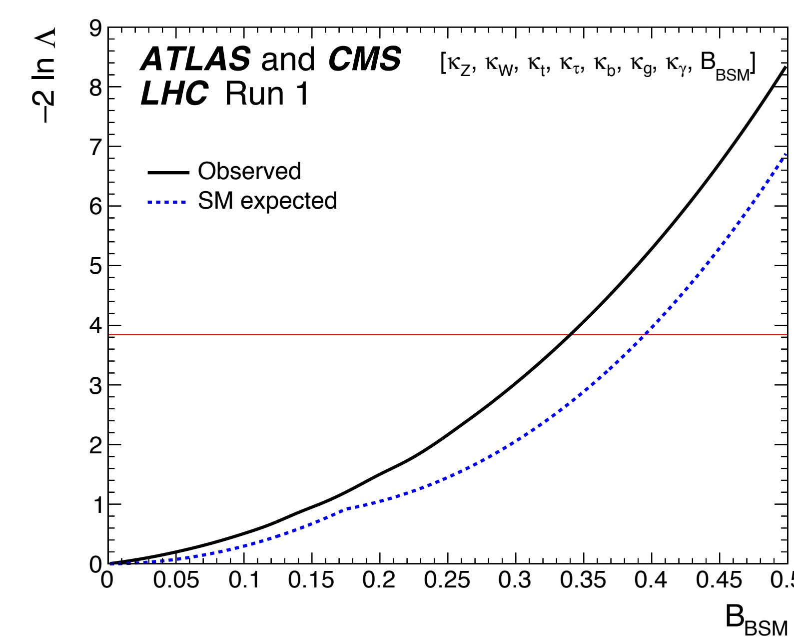

- **Rare decays provide novel probes to new physics**

Coverage of this talk

- Invisible decay of the Higgs boson
  - VBF production, CMS-HIG-17-023, accepted by PLB
- Higgs boson decay in the μμ final state
  - Published at PRL 122 021801
- Higgs boson decay in the llγ final state
  - $H \to Z/\gamma^* + \gamma \to ll\gamma$, l = μ or e, published at JHEP 11 (2018) 152
  - $H(Z) \to J/\psi\gamma \to \mu\mu\gamma$, published at EPJC 79 (2019)94
- Higgs (Z) boson decay in the J/ψ or ϒ(nS) pairs final state
  - CMS-PAS-HIG-18-025

H→Invisible

- Only via $H \to ZZ^* \to 4\nu$ in SM, with BR~0.1%
- The rate of H→Invisible may be enhanced in several BSM scenarios
  - For example, one postulates that the Higgs boson acts as a portal between dark matter and SM sector

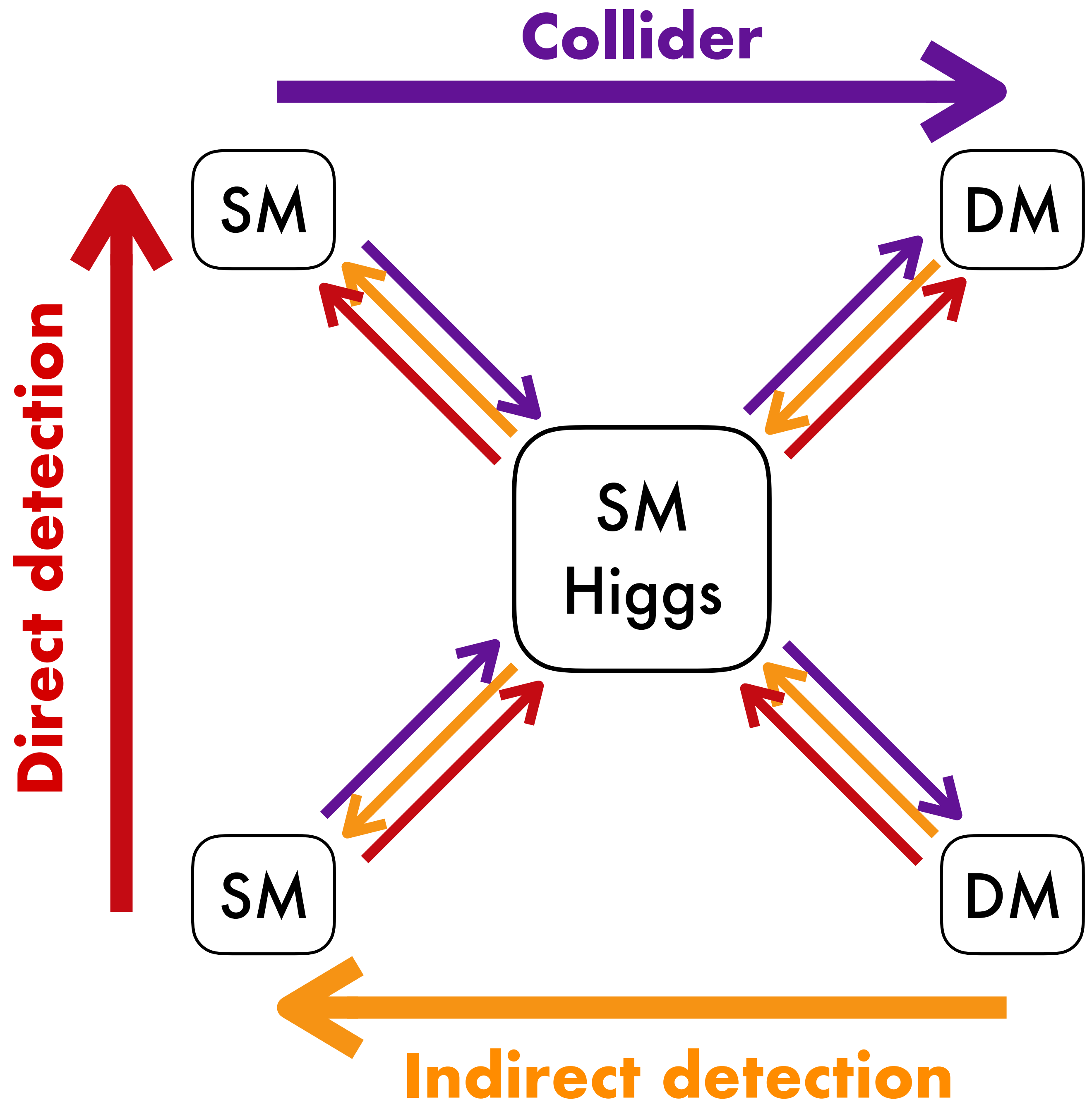

H→Invisible in VBF

- Event signatures of the VBF production are exploited – two jets with large separation in η and with large m_{jj}
  - ~95% of background is from V+jets processes, $Z(\nu\bar{\nu})$+jets and $W(l\nu)$+jets → can be discriminated/suppressed by requiring large m_{jj} and $|\Delta\eta_{jj}|$
- Expected signal ~3 assuming $BR_{SM}(H\rightarrow inv)$, along with much larger background (> 4 order of magnitude than expected signal)
- **M_{jj}-based analysis**, leading to **an obs. (exp.) upper limit (UL) on BR(H→inv) of 0.33 (0.25)**

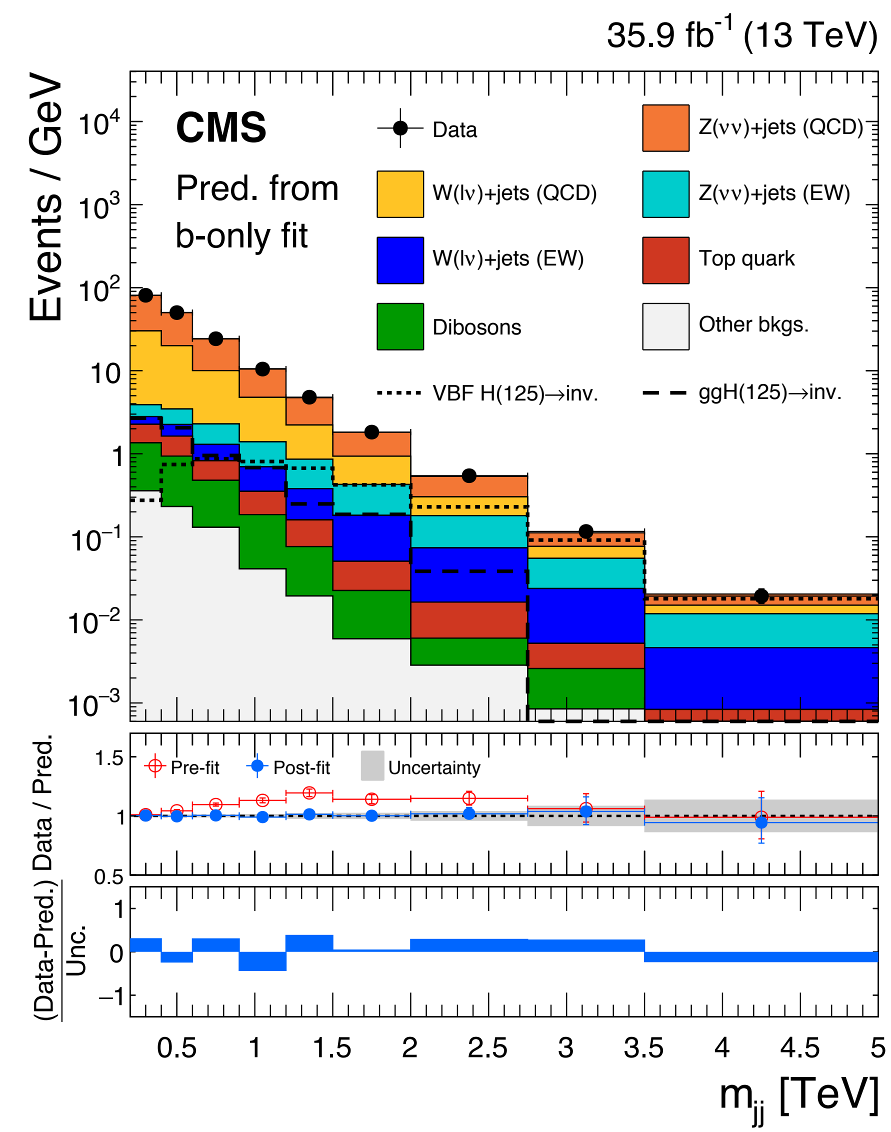

H→Invisible – combination

- A combination with searches utilizing VH and ggF productions using 2016 data is performed
  - **An obs.(exp.) UL on BR(H→inv) of 0.26 (0.20)** is obtained
  - (Events that overlap with the VBF analysis are removed in the combination)

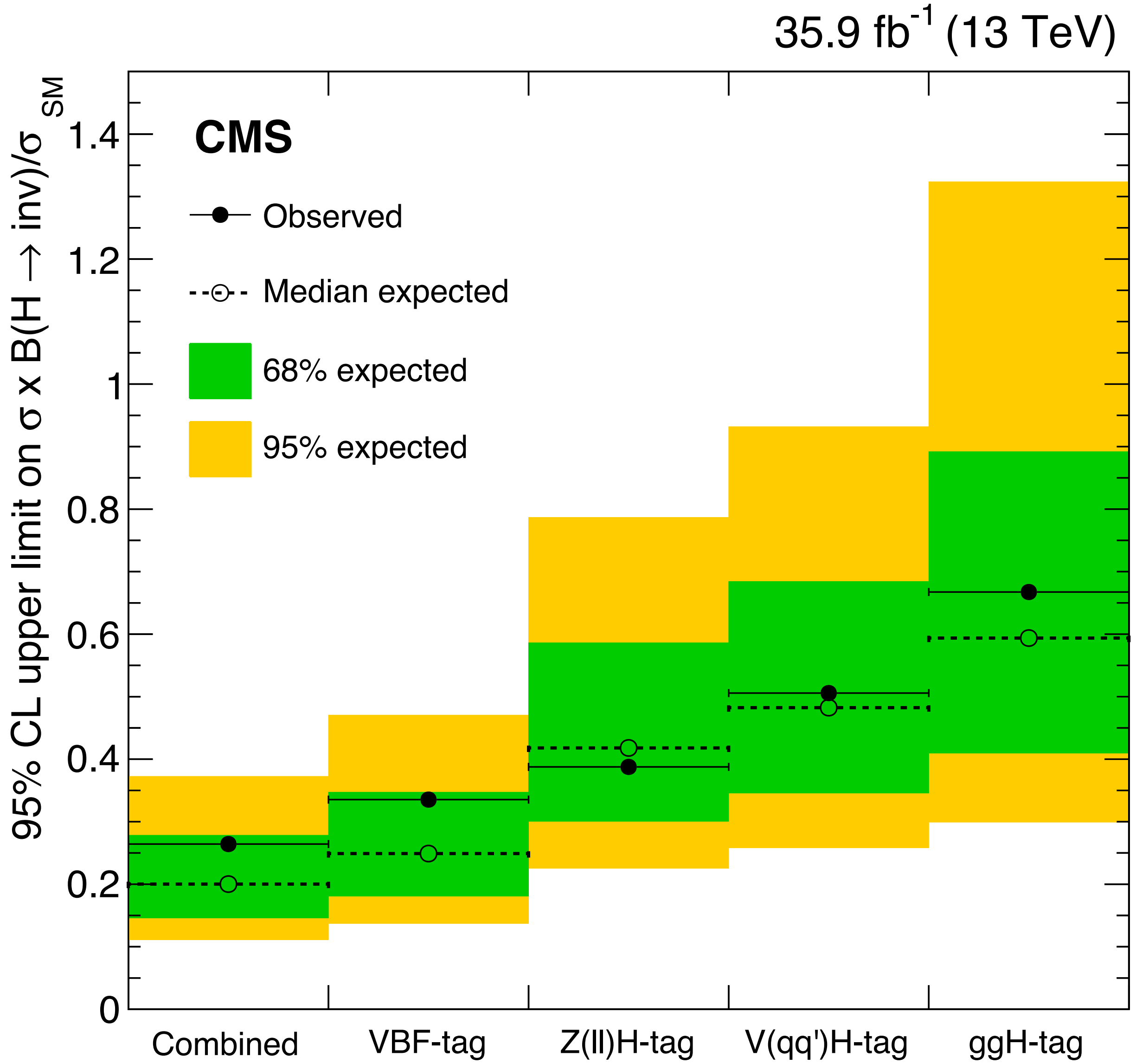

Analysis	Final state	Signal composition	Observed limit	Expected limit
VBF-tag	VBF-jet + p_T^{miss}	52% VBF, 48% ggH	0.33	0.25
VH-tag	$Z(\ell\ell) + p_T^{miss}$	79% qqZH, 21% ggZH	0.40	0.42
	V(qq') + p_T^{miss}	39% ggH, 6% VBF, 33% WH, 22% ZH	0.50	0.48
ggH-tag	jets + p_T^{miss}	80% ggH, 12% VBF, 5% WH, 3% ZH	0.66	0.59

H→Invisible – combination

- A combination of searches using data collected at $\sqrt{s}$=7, 8, 13 TeV is performed
  - **An obs.(exp.) UL on BR(H→inv) of 0.19 (0.15)** is obtained
  - Interpretation on Higgs portal model: the most stringent limits for dark matter mass m_χ smaller than 18 (7) GeV, assuming the DM candidate considered being fermion (scalar)-like (following the discussion in arXiv:1112.3299)

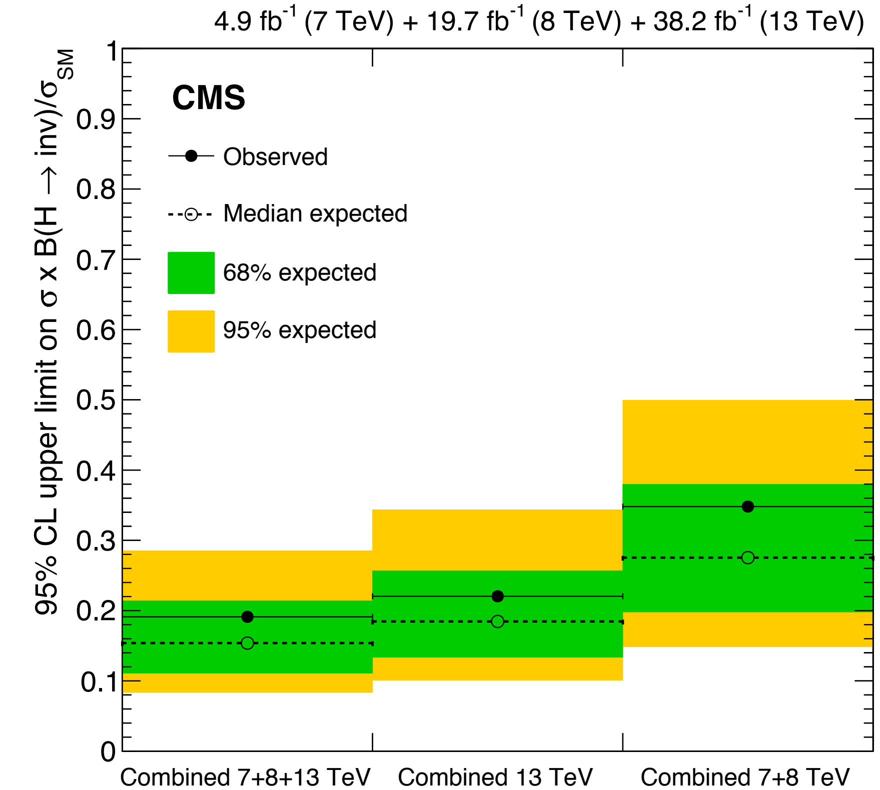

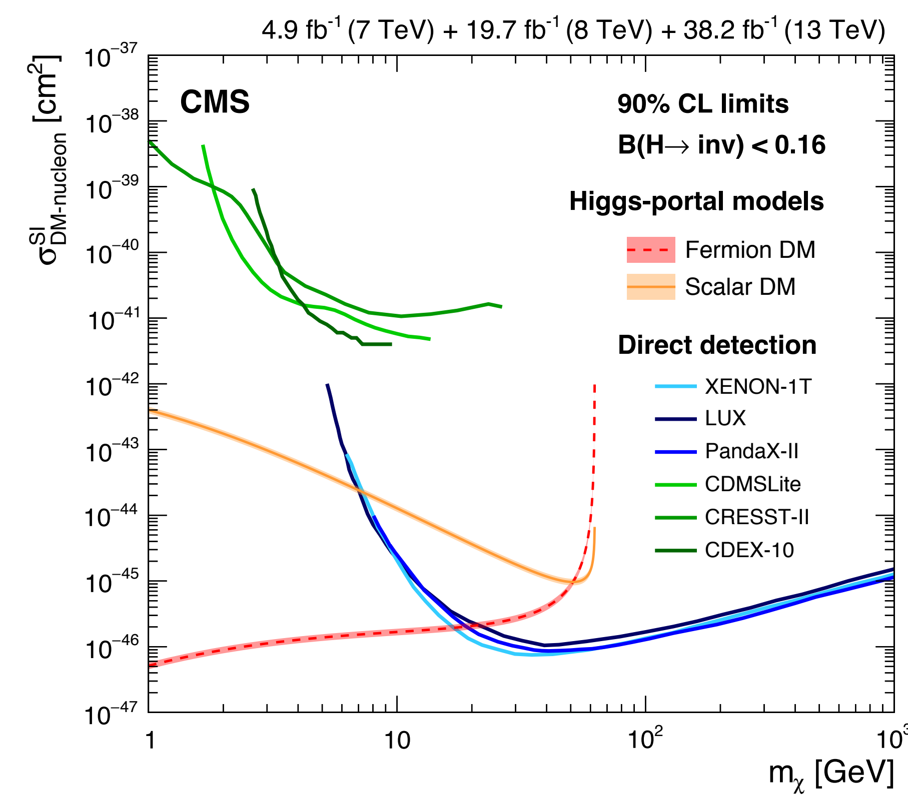

$H \to \mu\mu$

- The direct probe to Higgs coupling with 2nd generation of fermion
  - $H \to \mu\mu$ is the only accessible one in LHC
- $BR_{SM} = 2.2 \times 10^{-4}$, owing to the small H-μ coupling
- Experimentally clean & good mass resolution
  - Signal would appear as a peak in $m_{\mu\mu}$ on top of smoothly falling distribution that mainly consists of Drell-Yan process and $t\bar{t}$ production with leptonic decay

$H\to\mu\mu$

- Expected signal yield ~250, while the expected background (raw count) at $m_{\mu\mu}$@125 GeV ~O(10^4)
- Boost decision tree (BDT) is exploited. The BDT score and expected $m_{\mu\mu}$ resolution are used for event categorization
- **$m_{\mu\mu}$ is used as the signal/background discriminating variable** in the hypothesis test, where signal/background shapes are modeled by parametrized functions

	Obs. (exp.) UL on σ/σ_{SM}	Obs. (exp.) significance
2016 data	**3.0 (2.5)**	**0.6 (0.9)σ**
7+8+13 TeV data	**2.9 (2.2)**	**0.9 (1.0)σ**

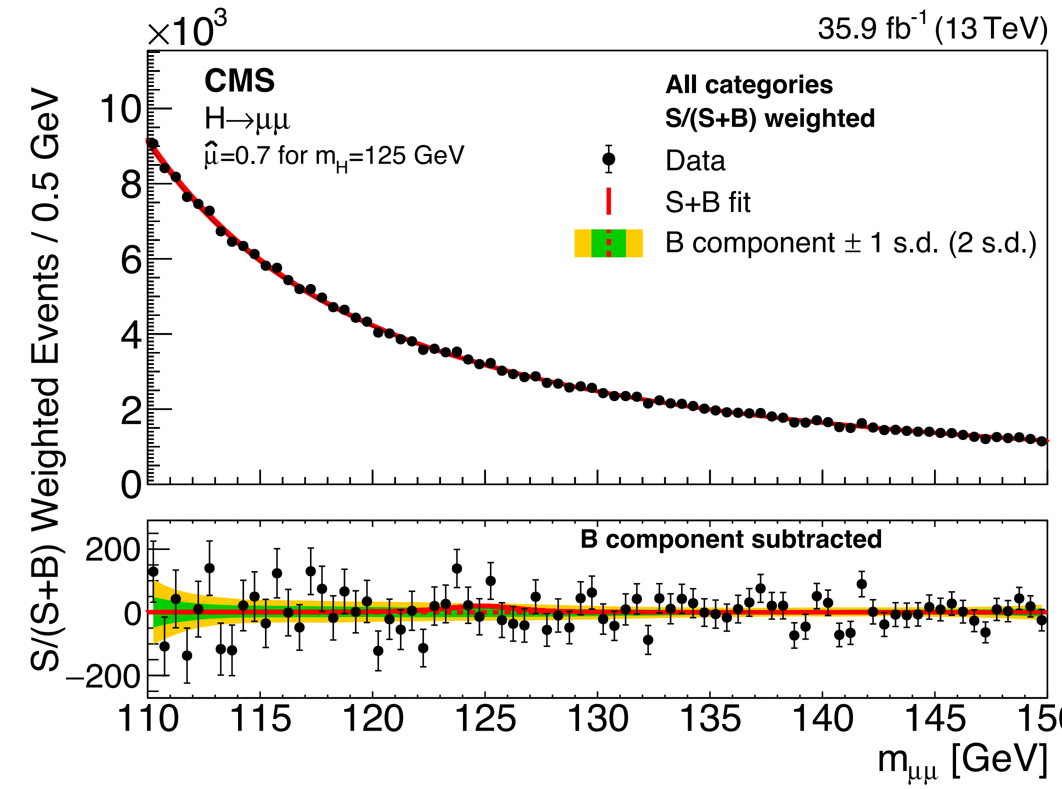

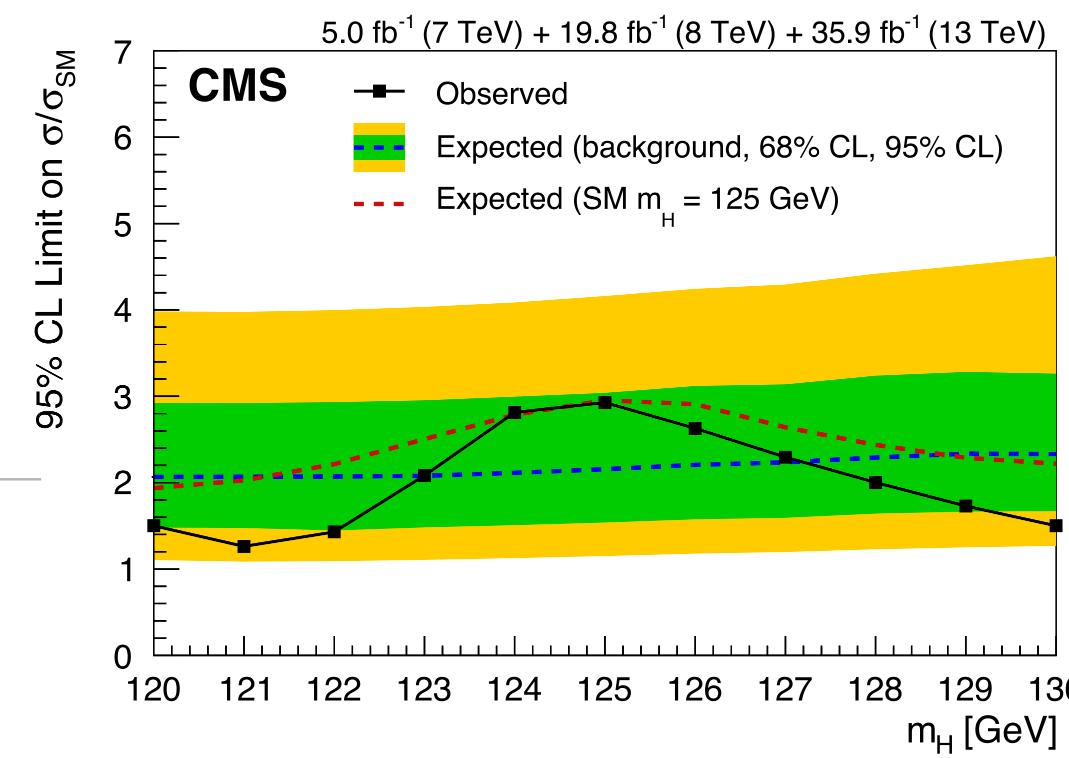

Higgs decay in the llγ final state

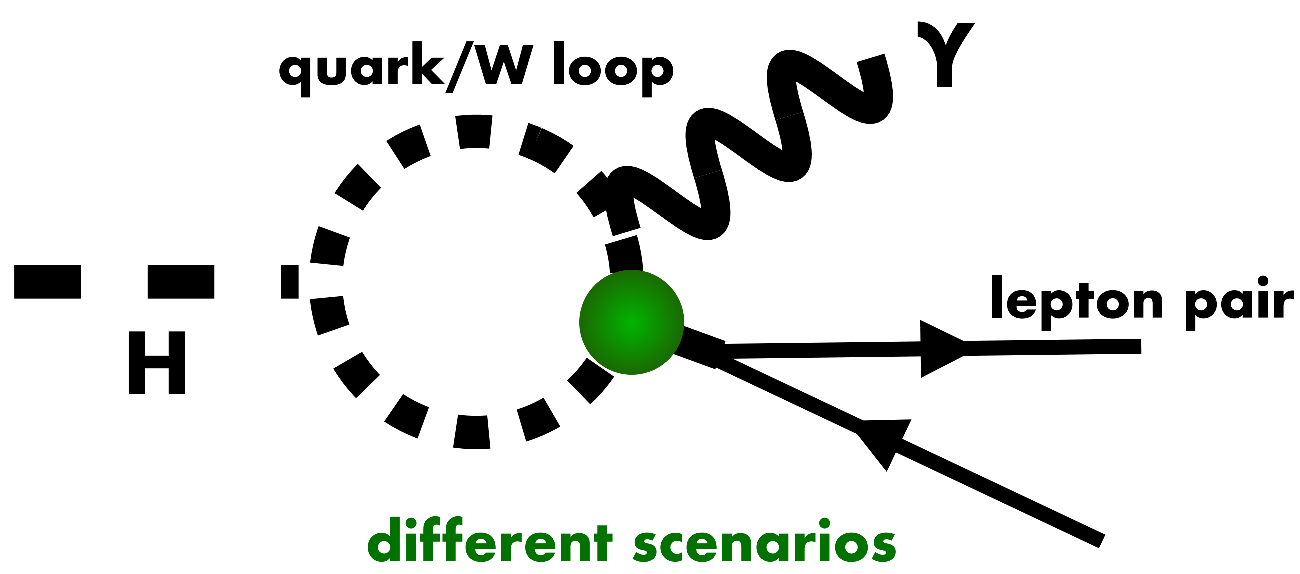

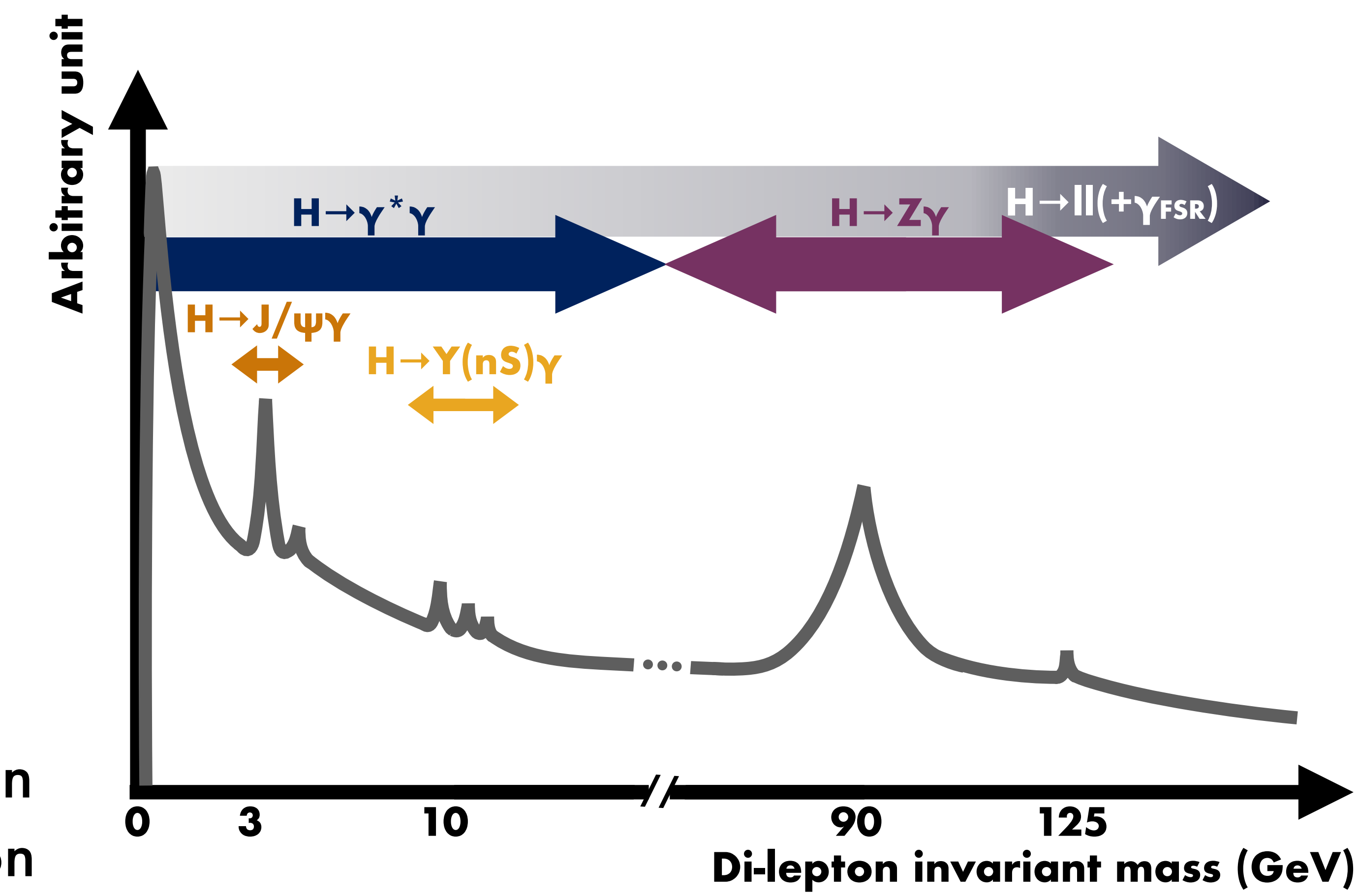

✦ Same-flavor Lepton pair and an isolated photon
→ experimentally clean & good mass resolution

Scenario	
charm quarks hardronize to form J/ψ	direct amplitude of H→J/ψγ
quark/W loop to Z/γ*	H→ Z/γ*+γ
quark/W loop to γ*, then γ*converts into J/ψ	indirect amplitude of H→J/ψγ

Higgs decay in the $ll\gamma$ final state

- $H \rightarrow Z/\gamma^*\gamma$
  - Loop-induced diagrams, new physics present in the loop will modify the decay rates
  - Provide additional test for the CP property of the Higgs boson, as indicated in e.g. arXiv:1408.0342
  - One of the most promising channels among rare decays of the Higgs boson
  - $BR_{SM}(H \rightarrow Z\gamma) \simeq 1.5\times10^{-3}$, $BR_{SM}(H \rightarrow \gamma^*\gamma \rightarrow \mu\mu\gamma) \simeq 3.8\times10^{-5}$
- $H/Z \rightarrow J/\psi\gamma$
  - Rare decay, $BR_{SM}(H \rightarrow J/\psi\gamma) \simeq 3.0\times10^{-6}$
  - Deviation of the $Hc\bar{c}$ coupling from SM leads to changes in the BR
  - Extensions of the SM modify the $Hc\bar{c}$ coupling → interesting in terms of BSM
  - A similar search on $Z \rightarrow J/\psi\gamma$ is jointly performed; $BR_{SM}(Z \rightarrow J/\psi\gamma) \simeq 9.0\times10^{-8}$

H→Z/γ*γ→llγ

- Two well-identified leptons originated from PV & Energetic & isolated photon

Order of categorization ↓

	H→Zγ	H→γ*γ	
	Lepton tag	–	VH & ttH production
	Di-jet tag	Di-jet tag	VBF production
	Boosted tag	–	A boosted Higgs boson recoiling against a jet
	4 Untagged categories	3 Untagged categories	Based on photon η_{SC} & R9 variable

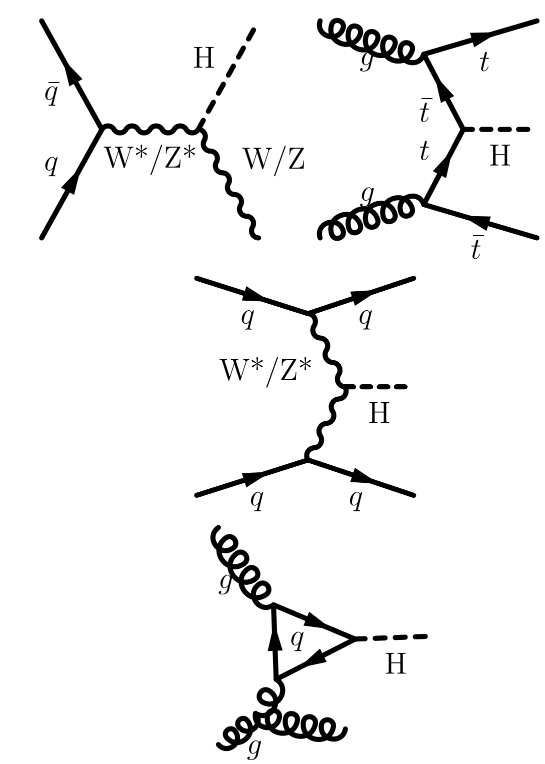

- H→Zγ→llγ: expected signal yield O(50), is at the same order as H→4l, but with much larger irreducible backgrounds O(>10^4)
- H→γ*γ→μμγ: smaller signal yield O(20), and also smaller background O(>10^3) than H→Zγ owing to the special event signature

H→Z/γ*γ→llγ

✦ **$m_{ll\gamma}$ as the signal/background discriminating variable** in the hypothesis test

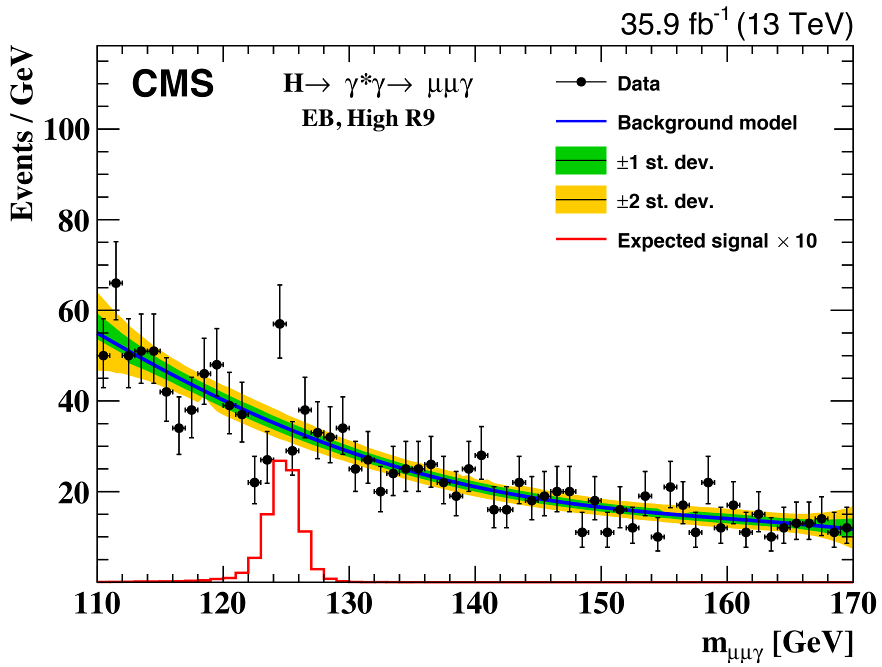

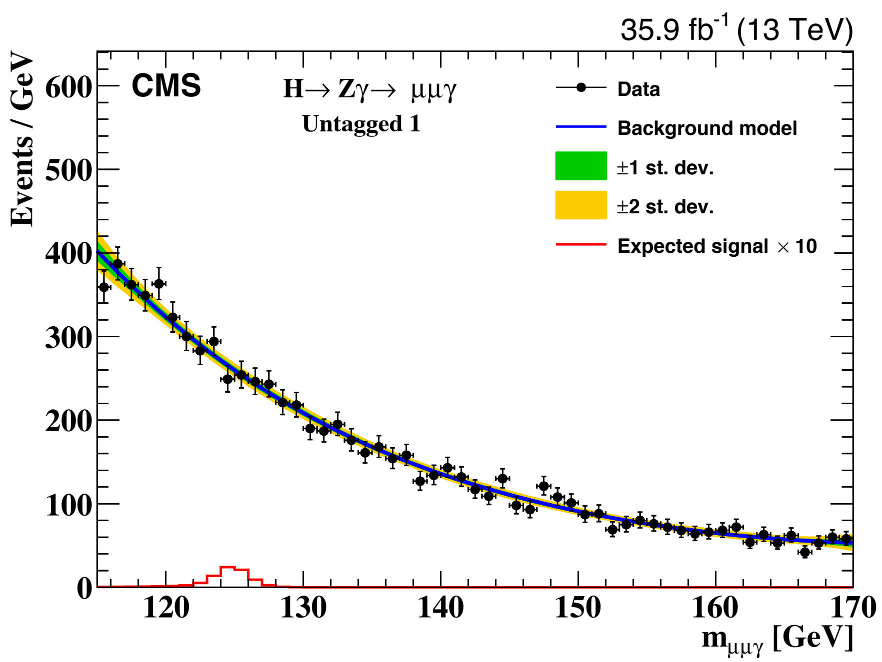

★ Simulated events of backgrounds are not overlaid in the plots!

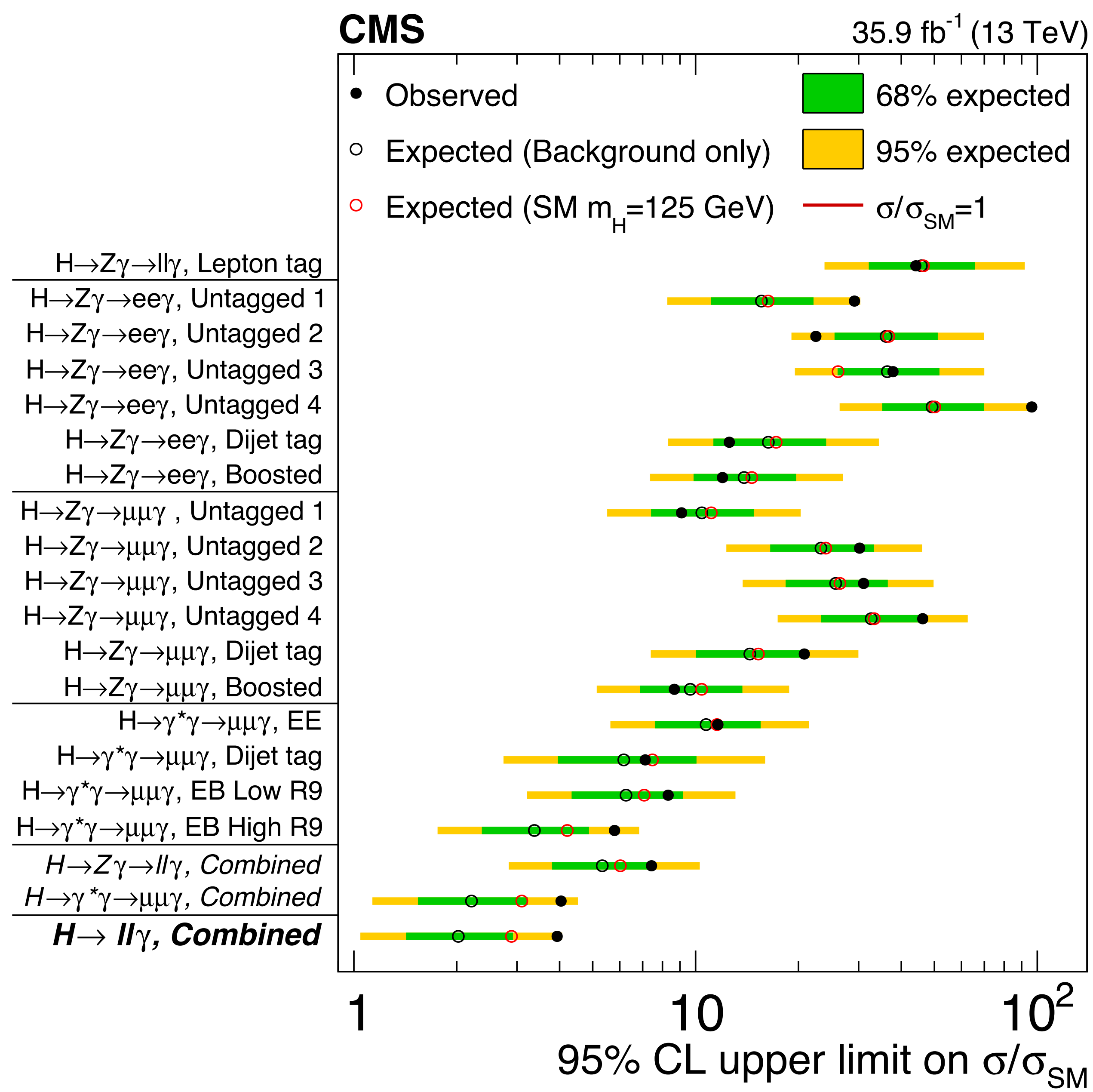

✦ **Obs. (exp.) upper limit for σ/σ_{SM} is 3.9 (2.0), with corresponding significance of ~2σ (1σ)**

H/Z→J/ψ γ→μμγ

✦ **$m_{\mu\mu\gamma}$ as the signal/background discriminating variable** in the hypothesis test

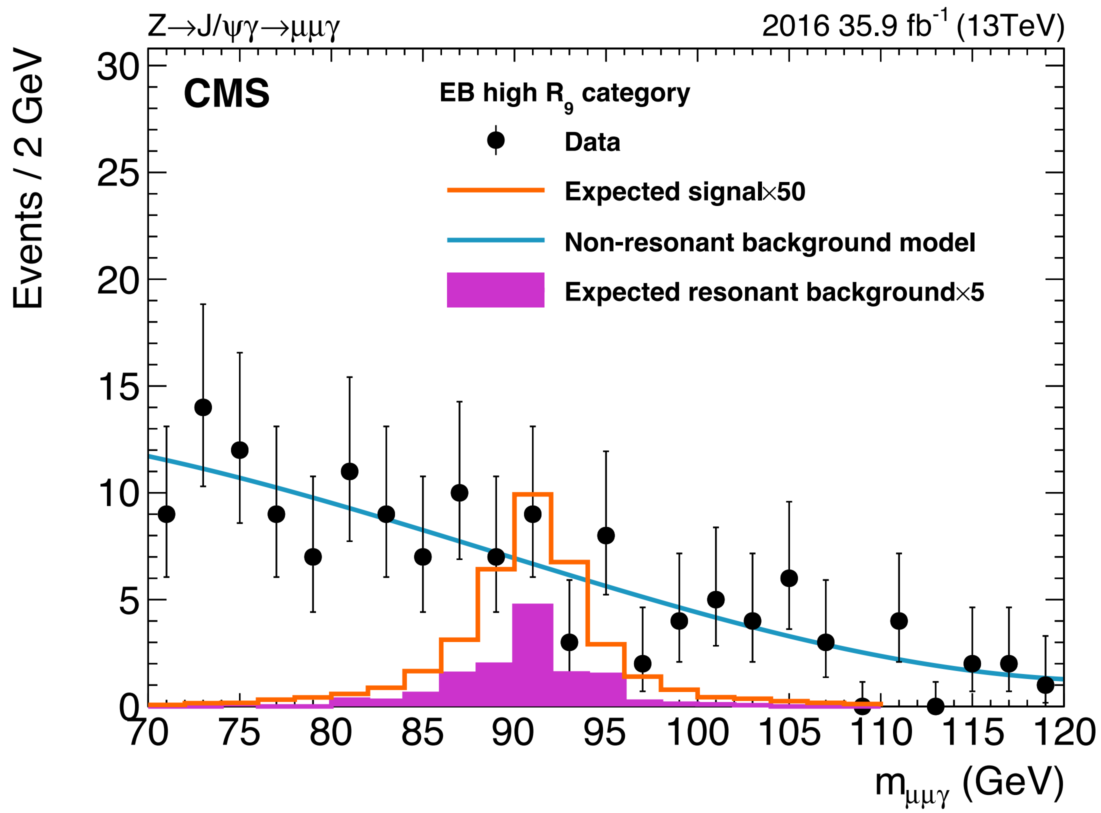

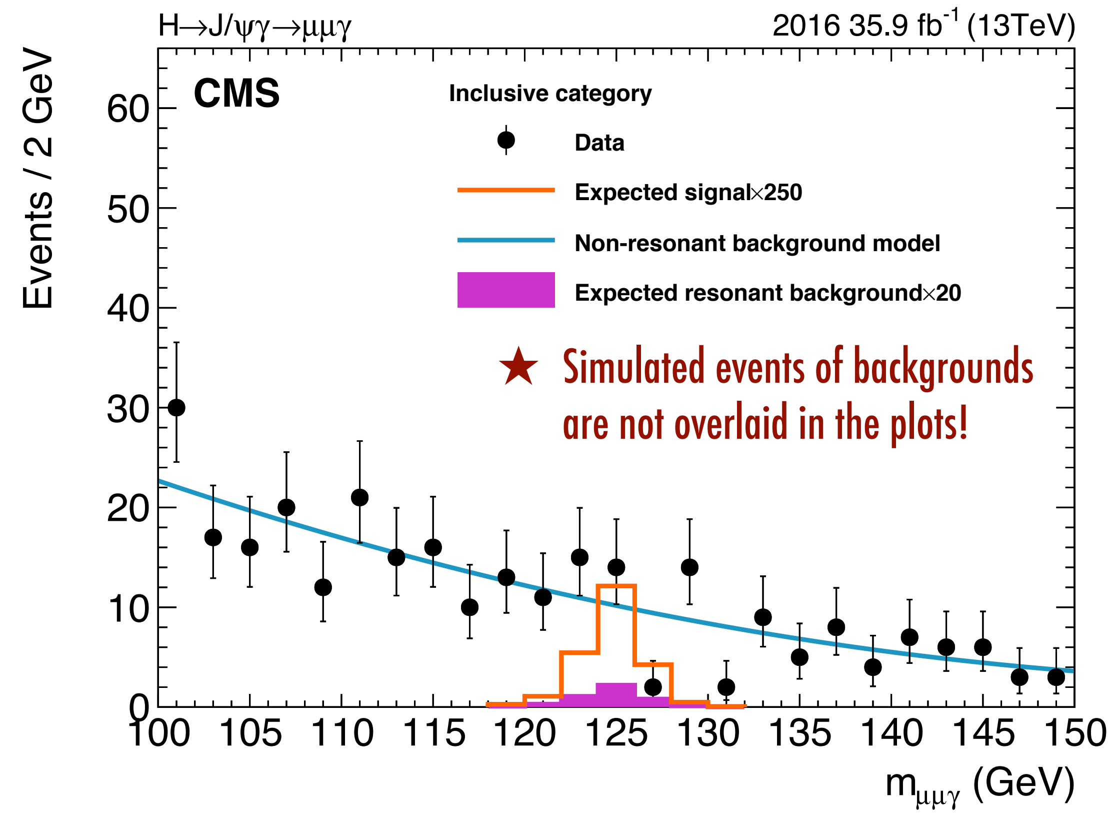

	Obs. (exp.) upper limit @ m_H=125GeV	
Channel	BR	BR/BR_{SM}
Z→J/ψγ	**1.4(1.6)E-6**	**15 (17)**
H→J/ψγ	**7.6(5.2)E-4**	**260 (170)**
	Combination with CMS Run1 result leads to an UL of **220 (160)**×SM prediction	

H/Z→meson+meson→4μ

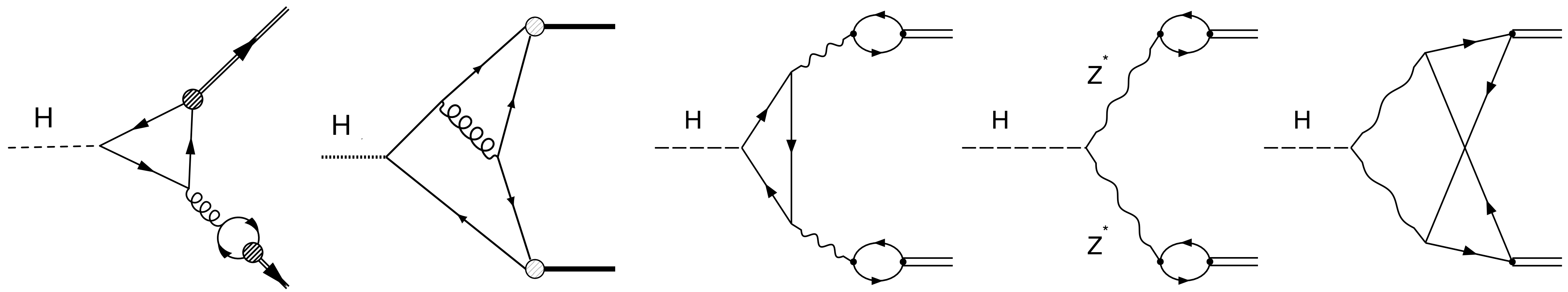

Leading order Feynman diagrams for H→QQ, with Q=J/ψ and Υ

- Latest SM prediction: $BR_{SM}(H\to J/\psi J/\psi)\simeq 1.5\times 10^{-10}$; $BR_{SM}(H\to \Upsilon\Upsilon)\simeq 2\times 10^{-9}$
- Similar to H→J/ψγ, the channel provides an alternative way to probe $Hc\bar{c}$ coupling
- A similar search on Z→QQ is jointly performed; $BR_{SM}(Z\to J/\psi J/\psi)\approx 10^{-12}$; $BR_{SM}(Z\to \Upsilon\Upsilon)$ does not have public calculation yet
- First search for the Higgs boson decaying into quarkonium pair

H/Z→meson+meson→4μ

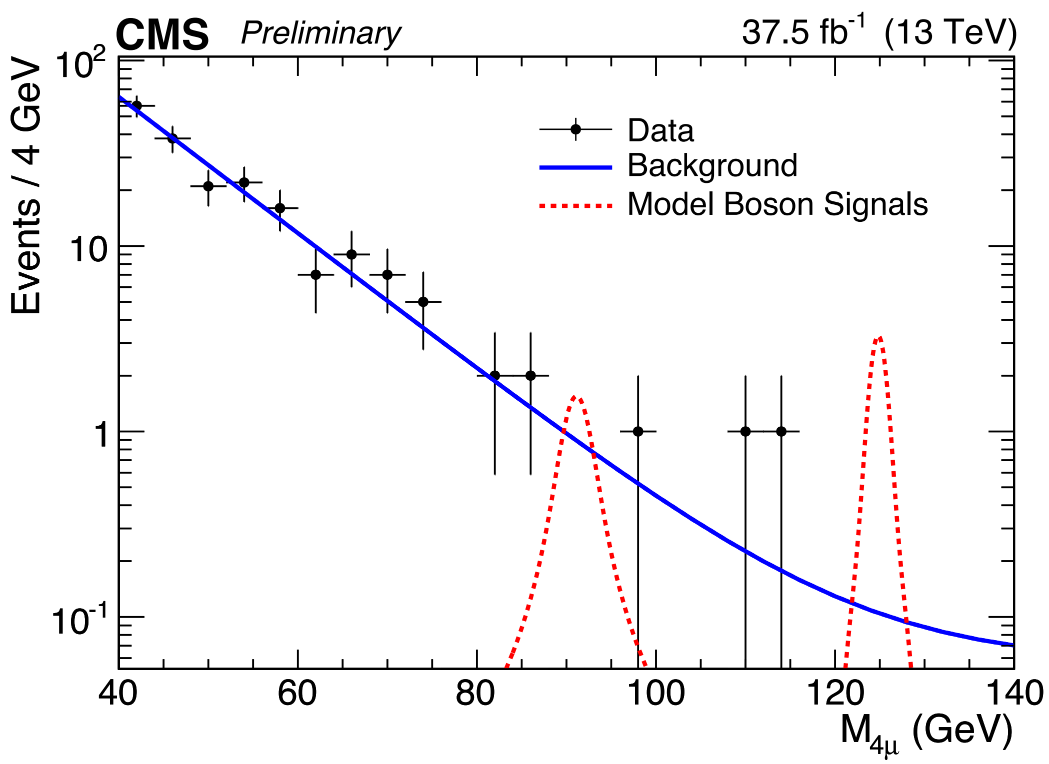

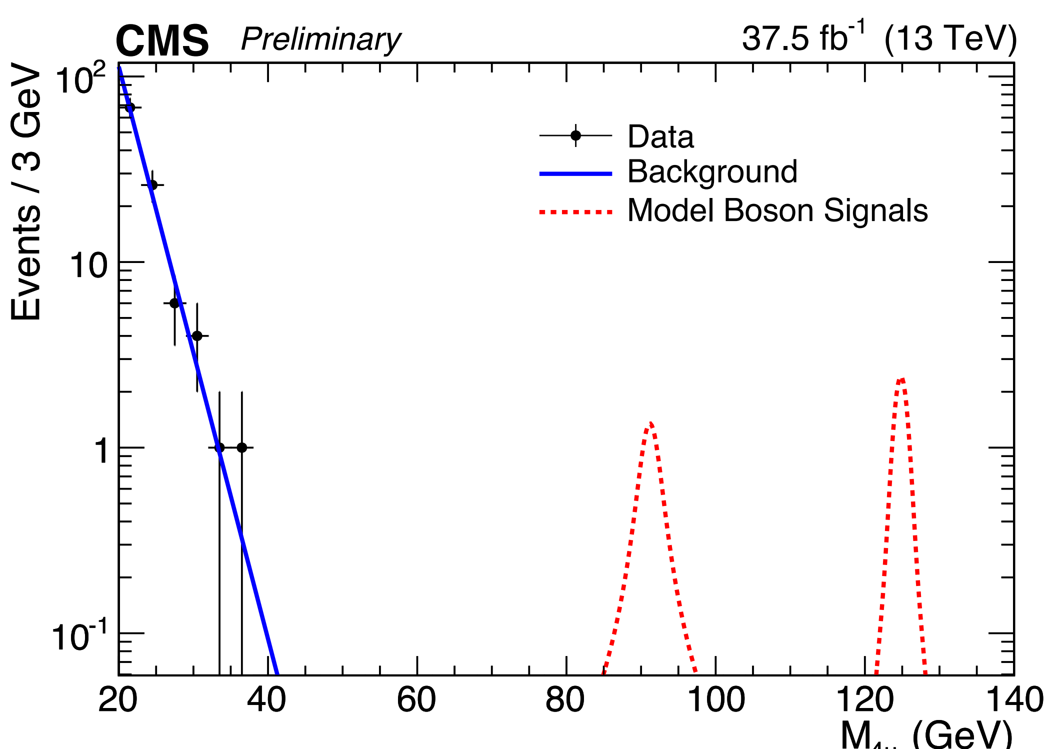

- Four well-identified leptons to form two Q candidates that compatible with J/ψ or ϒ

✦ **$m_{4\mu}$ is used as the signal/background discriminating variable** in the hypothesis test

- The analysis does not distinguish the three ϒ(nS) states. Possibility of the ϒ feed-down is properly taken in account

	observed	expected
$\mathcal{B}(\mathrm{H} \to \mathrm{J}/\psi \mathrm{J}/\psi) \times 10^3$	1.8	$1.8^{+0.2}_{-0.1}$
$\mathcal{B}(\mathrm{H} \to \Upsilon\Upsilon) \times 10^3$	1.4	1.4 ± 0.1
$\mathcal{B}(\mathrm{Z} \to \mathrm{J}/\psi \mathrm{J}/\psi) \times 10^6$	2.2	$2.8^{+1.2}_{-0.7}$
$\mathcal{B}(\mathrm{Z} \to \Upsilon\Upsilon) \times 10^6$	1.5	1.5 ± 0.1

Summary

- A large campaign of searches for rare decays of the Higgs boson has been conducted since the discovery of the Higgs boson. So far, all searches are consistent with the SM prediction

- Observed (expected) upper limits on

  (1) **BR($H\to inv$)~0.19 (0.15)** in combination with Run-1 results

  (2) **BR($H\to\mu\mu$)~2.9 (2.2)×SM prediction** in combination with Run-1 results

  (3) **BR($H\to Z/\gamma^*\gamma\to ll\gamma$)~3.9 (2.0)×SM prediction** (comparable to Hμμ search)

  (4) **BR($H\to J/\psi\gamma$)~220 (160)×SM prediction** in combination with Run-1 result
  BR($Z\to J/\psi\gamma$)~15(17)×SM prediction (comparable to HH search)

  (5) **BR($H\to QQ$)≳O(10^6)×SM prediction** (first search of this kind)

- More data are required to approach the SM sensitivity. Meanwhile, advanced analysis techniques are being developed

Backup

■ CMS-HIG-17-031, submitted EPJC

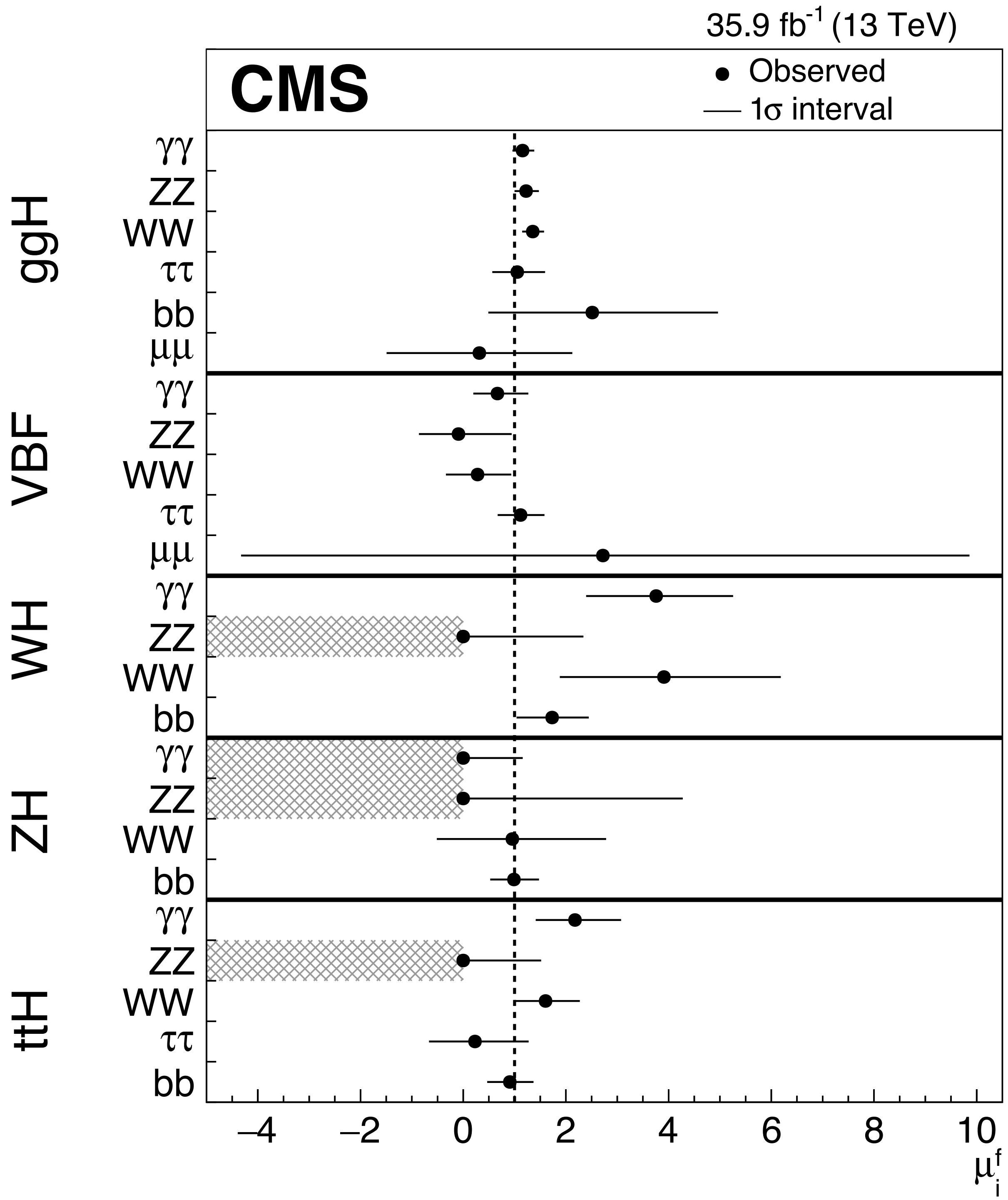

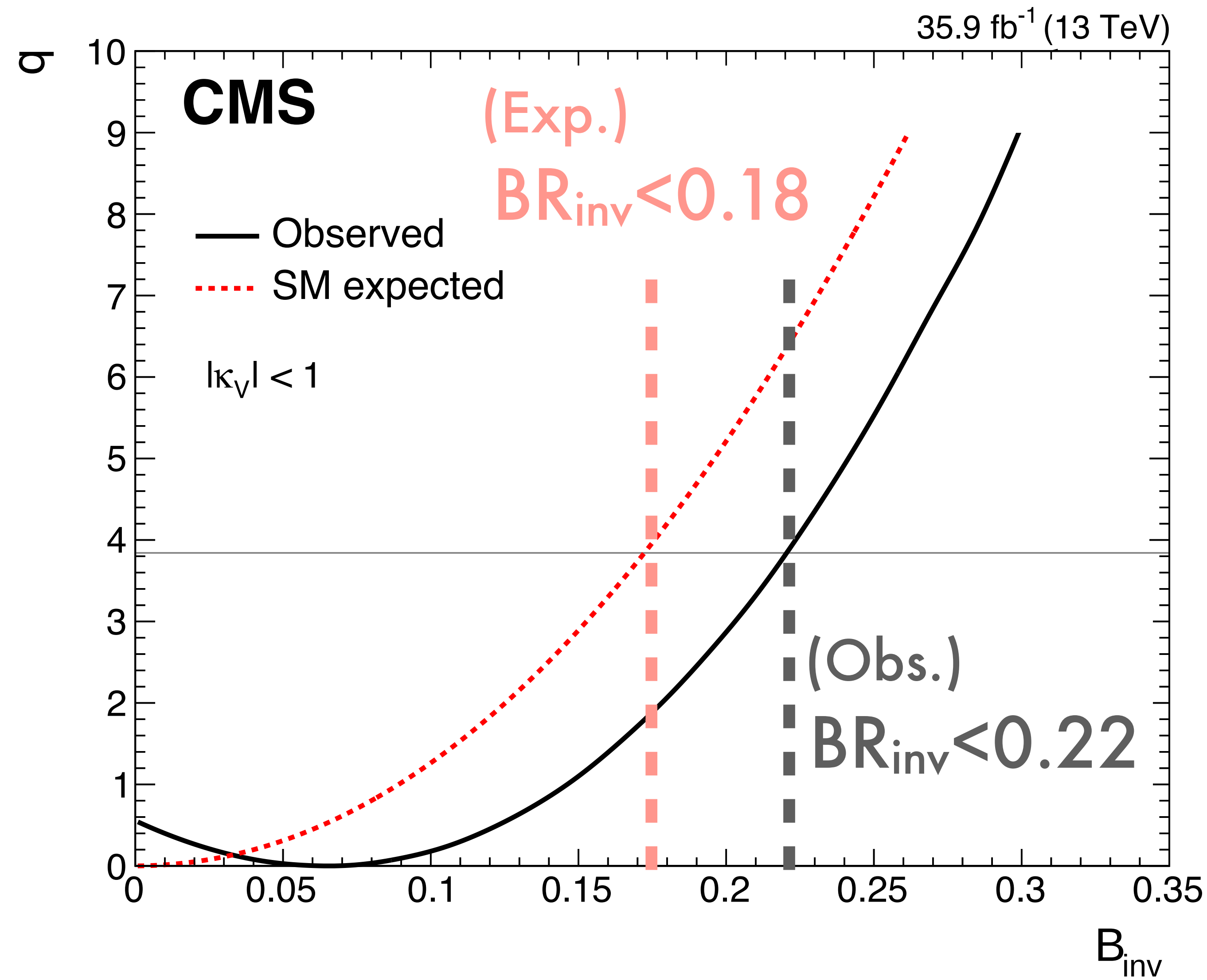

(Obs.) BR_{undet}<0.38

* The total branching fraction to any final state that is not detected by the channels

ATLAS-CONF-2019-005

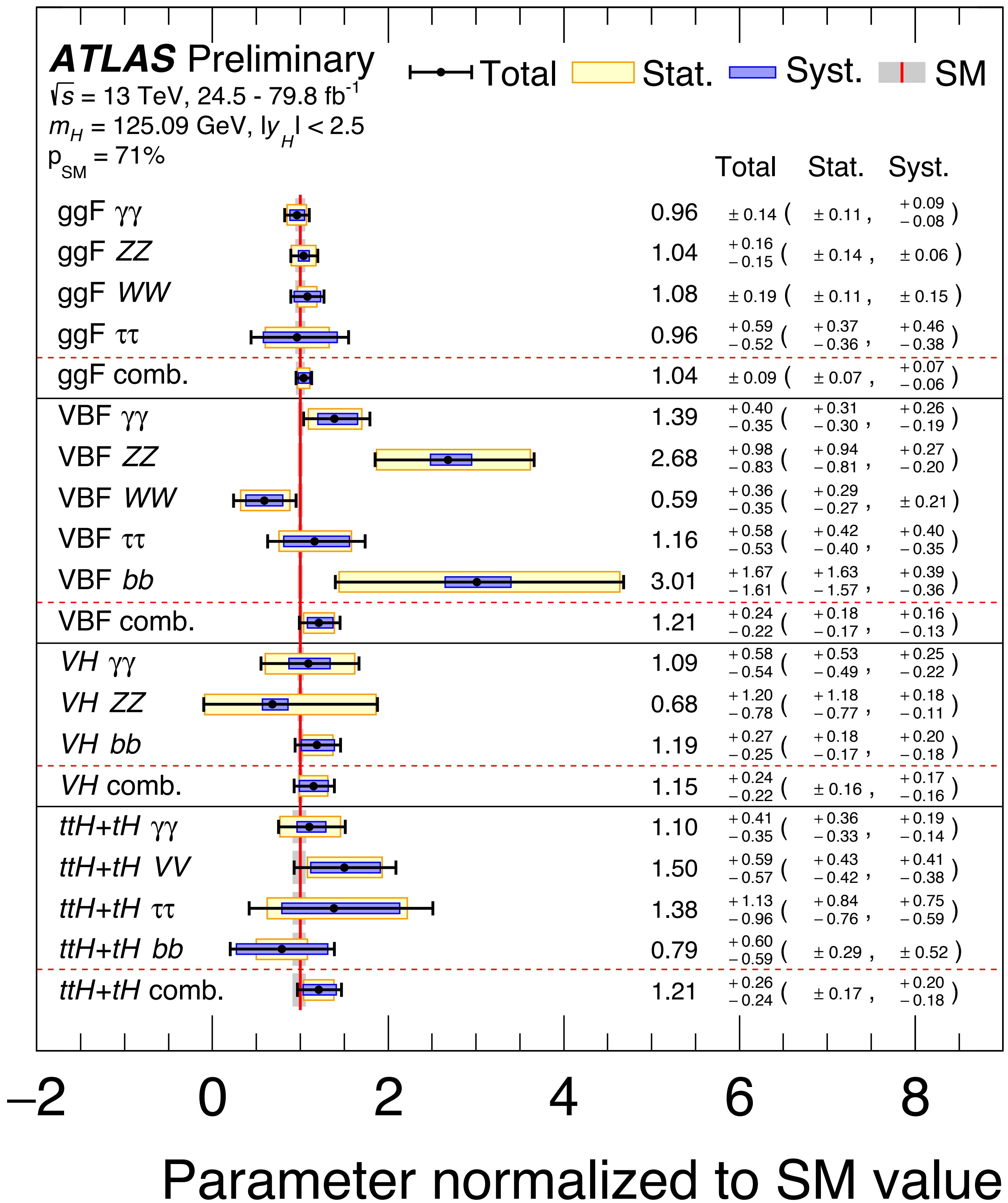

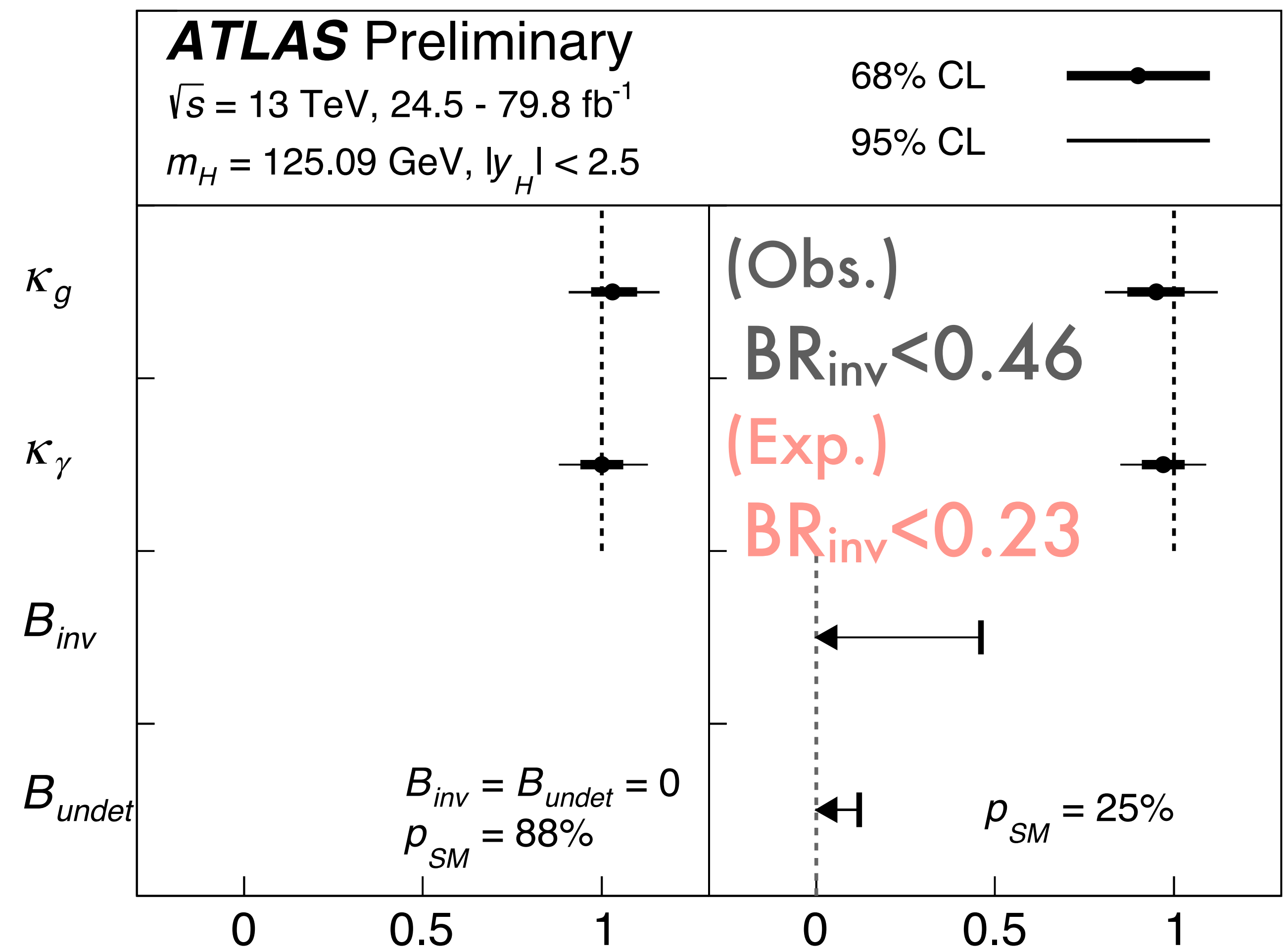

(Obs.) $BR_{undet}<0.12$

(Exp.) $BR_{undet}<0.32$

* The total branching fraction to any final state that is not detected by the channels

Coverage of this talk

- Invisible decay of the Higgs boson
  - VBF production, CMS-HIG-17-023, accepted by PLB
- Higgs boson decay in the $\mu\mu$ final state
  - Published at PRL 122 021801
- Higgs boson decay in the $ll\gamma$ final state
  - $H \to Z/\gamma^* + \gamma \to ll\gamma$, $l = \mu$ or e, published at JHEP 11 (2018) 152
  - $H(Z) \to J/\psi\gamma \to \mu\mu\gamma$, published at EPJC 79 (2019)94
- Higgs (Z) boson decay in the J/ψ or $\Upsilon(nS)$ pairs final state
  - CMS-PAS-HIG-18-025

H→Invisible in VBF

- A comparison of the shapes of the key discriminating observables for signal and V+jets background
  - Both EW and QCD productions are shown

EW **QCD**

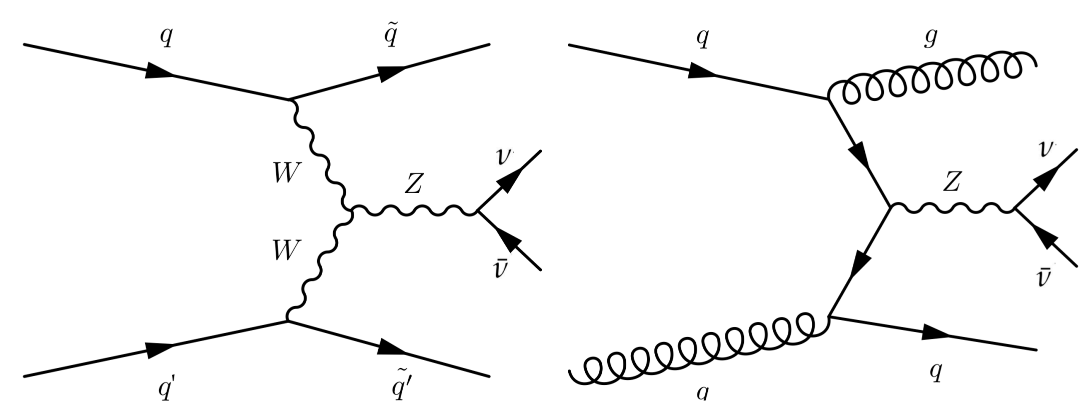

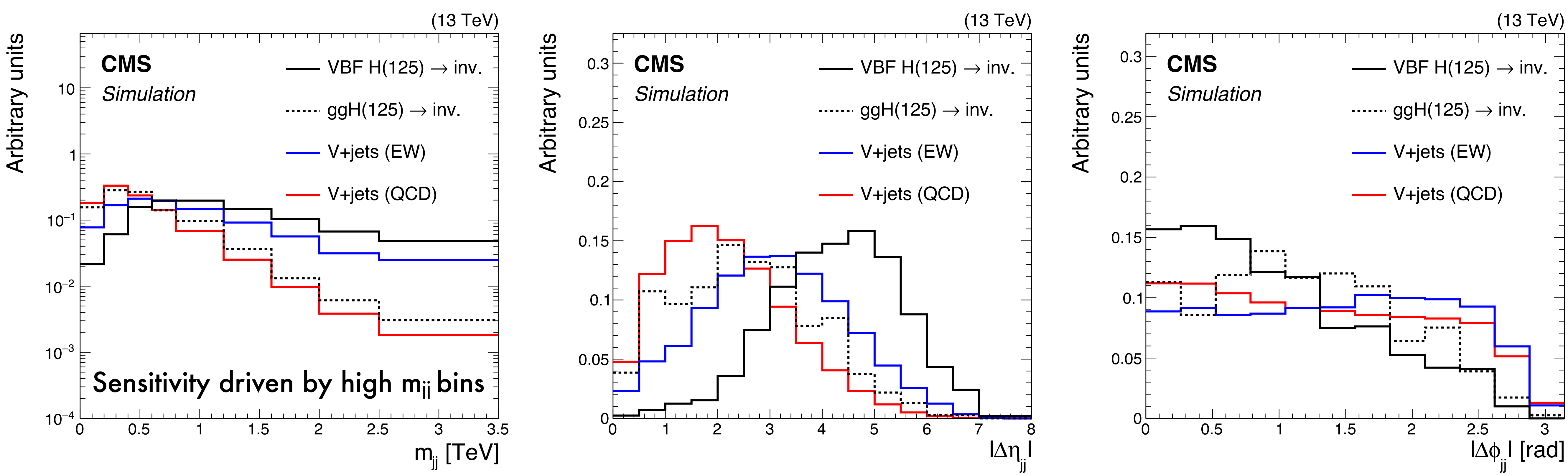

H→Invisible in VBF

- Summary of the kinematic selections used to define the SR for both the shape and the cut-and-count analyses

Observable	Shape analysis	Cut-and-count analysis	Target background
Leading (subleading) jet	$p_{\mathrm{T}} > 80\,(40)$ GeV, $\lvert\eta\rvert < 4.7$		All
$p_{\mathrm{T}}^{\mathrm{miss}}$	>250 GeV		QCD multijet, $\mathrm{t\bar{t}}$, γ+jets, V+jets
$\Delta\phi(\vec{p}_{\mathrm{T}}^{\mathrm{miss}}, \vec{p}_{\mathrm{T}}^{\mathrm{jet}})$	>0.5 rad		QCD multijet, γ+jets
Muons (electrons)	$\mathrm{N}_{\mu,\mathrm{e}} = 0$ with $p_{\mathrm{T}} > 10$ GeV, $\lvert\eta\rvert < 2.4\,(2.5)$		$\mathrm{W}(\ell\nu)$+jets
τ_{h} candidates	$\mathrm{N}_{\tau_{\mathrm{h}}} = 0$ with $p_{\mathrm{T}} > 18$ GeV, $\lvert\eta\rvert < 2.3$		$\mathrm{W}(\ell\nu)$+jets
Photons	$\mathrm{N}_{\gamma} = 0$ with $p_{\mathrm{T}} > 15$ GeV, $\lvert\eta\rvert < 2.5$		γ+jets, $\mathrm{V}\gamma$
b quark jet	$\mathrm{N}_{\mathrm{jet}} = 0$ with $p_{\mathrm{T}} > 20$ GeV, CSVv2 > 0.848		$\mathrm{t\bar{t}}$, single top quark
$\eta_{\mathrm{j1}}\,\eta_{\mathrm{j2}}$	<0		$\mathrm{Z}(\nu\bar{\nu})$+jets, $\mathrm{W}(\ell\nu)$+jets
$\lvert\Delta\phi_{\mathrm{jj}}\rvert$	<1.5 rad		$\mathrm{Z}(\nu\bar{\nu})$+jets, $\mathrm{W}(\ell\nu)$+jets
$\lvert\Delta\eta_{\mathrm{jj}}\rvert$	>1	>4	$\mathrm{Z}(\nu\bar{\nu})$+jets, $\mathrm{W}(\ell\nu)$+jets
m_{jj}	>200 GeV	>1.3 TeV	$\mathrm{Z}(\nu\bar{\nu})$+jets, $\mathrm{W}(\ell\nu)$+jets

H→Invisible in VBF

- Expected event yields in each m_{jj} bin for signal and various background processes in the SR of the shape analysis.

Process	m_{jj} range in TeV								
	0.2–0.4	0.4–0.6	0.6–0.9	0.9–1.2	1.2–1.5	1.5–2.0	2.0–2.75	2.75–3.5	> 3.5
$Z(\nu\nu)$ (QCD)	9311 ± 388	5669 ± 257	3884 ± 179	1648 ± 88	677 ± 42	405 ± 28	153 ± 14	22.8 ± 3.5	8.1 ± 2.2
$Z(\nu\nu)$ (EW)	201 ± 8	228 ± 10	273 ± 13	198 ± 11	129 ± 8	112 ± 8	70.6 ± 6.6	20.2 ± 3.1	10.8 ± 2.9
$W(\ell\nu)$ (QCD)	4755 ± 267	3017 ± 180	2090 ± 130	928 ± 63	361 ± 28	227 ± 19	80.4 ± 9.1	13.7 ± 2.7	4.5 ± 1.9
$W(\ell\nu)$ (EW)	102 ± 14	118 ± 16	133 ± 18	100 ± 13	61.2 ± 8.1	61.4 ± 7.6	39.4 ± 4.9	12.6 ± 1.9	5.6 ± 1.4
Top quark	208 ± 37	159 ± 28	119 ± 21	57.6 ± 10.2	28.7 ± 5.1	16.1 ± 2.9	8.9 ± 1.6	2.2 ± 0.4	0.7 ± 0.1
Dibosons	222 ± 39	157 ± 28	116 ± 21	48.2 ± 8.5	19.0 ± 3.4	9.3 ± 1.6	2.6 ± 0.5	1.4 ± 0.3	0.4 ± 0.1
Others	78.6 ± 19.5	51.0 ± 11.6	42.8 ± 11.5	13.6 ± 2.9	6.5 ± 1.5	3.3 ± 0.8	2.4 ± 0.6	0.7 ± 0.2	0.3 ± 0.4
Total bkg.	14878 ± 566	9401 ± 387	6658 ± 271	2994 ± 144	1283 ± 69	834 ± 51	358 ± 29	73.8 ± 9.4	30.3 ± 7.4
Signal	590 ± 244	559 ± 199	547 ± 151	447 ± 109	276 ± 58	304 ± 66	201 ± 36	68.6 ± 11.7	30.0 ± 6.4
Data	16177	10008	7277	3138	1439	911	408	87	29

- The expected signal contribution is calculated assuming BR(H→inv)=1
- The “Other backgrounds” includes QCD multijet and Z(ll)+jets backgrounds

H→Invisible in VBF

- Systematic uncertainties & their impacts on fitter signal strength

Source of uncertainty	Ratios	Uncertainty vs. m_{jj}	Impact on $\mathcal{B}(H \to inv)$
	Theoretical uncertainties		
Ren. scale V+jets (EW)	$Z(\nu\overline{\nu})/W(\ell\nu)$ (EW)	9–12%	48%
Ren. scale V+jets (QCD)	$Z(\nu\overline{\nu})/W(\ell\nu)$ (QCD)	9–12%	25%
Fac. scale V+jets (EW)	$Z(\nu\overline{\nu})/W(\ell\nu)$ (EW)	2–7%	4%
Fac. scale V+jets (QCD)	$Z(\nu\overline{\nu})/W(\ell\nu)$ (QCD)	2–7%	2%
PDF V+jets (QCD)	$Z(\nu\overline{\nu})/W(\ell\nu)$ (QCD)	0.5–1%	<1%
PDF V+jets (EW)	$Z(\nu\overline{\nu})/W(\ell\nu)$ (EW)	0.5–1%	<1%
NLO EW corr.	$Z(\nu\overline{\nu})/W(\ell\nu)$ (QCD)	1–2%	<1%
	Experimental uncertainties		
Muon reco. eff.	$Z(\mu\mu)/Z(\nu\overline{\nu})$, $W(\mu\nu)/W(\ell\nu)$	≈1%(per lepton)	8%
Electron reco. eff.	$Z(ee)/Z(\nu\overline{\nu})$, $W(e\nu)/W(\ell\nu)$	≈1%(per lepton)	3%
Muon id. eff.	$Z(\mu\mu)/Z(\nu\overline{\nu})$, $W(\mu\nu)/W(\ell\nu)$	≈1%(per lepton)	8%
Electron id. eff.	$Z(ee)/Z(\nu\overline{\nu})$, $W(e\nu)/W(\ell\nu)$	≈1.5%(per lepton)	4%
Muon veto	$Z(\nu\overline{\nu})/W(\ell\nu)$, W(CRs)$/W(\ell\nu)$	≈2.5 (2)% for EW (QCD)	7%
Electron veto	$Z(\nu\overline{\nu})/W(\ell\nu)$, W(CRs)$/W(\ell\nu)$	≈1.5 (1)% for EW (QCD)	5%
τ veto	$Z(\nu\overline{\nu})/W(\ell\nu)$, W(CRs)$/W(\ell\nu)$	≈3.5 (3)% for EW (QCD)	13%
Jet energy scale	Z (CRs)$/Z(\nu\overline{\nu})$, W(CRs)$/W(\ell\nu)$	≈1 (2)% for Z/Z (W/W)	4%
Electron trigger	$Z(ee)/Z(\nu\overline{\nu})$, $W(e\nu)/W(\ell\nu)$	≈1%	<1%
p_T^{miss} trigger	All ratios	≈2%	18%

H→Invisible in VBF

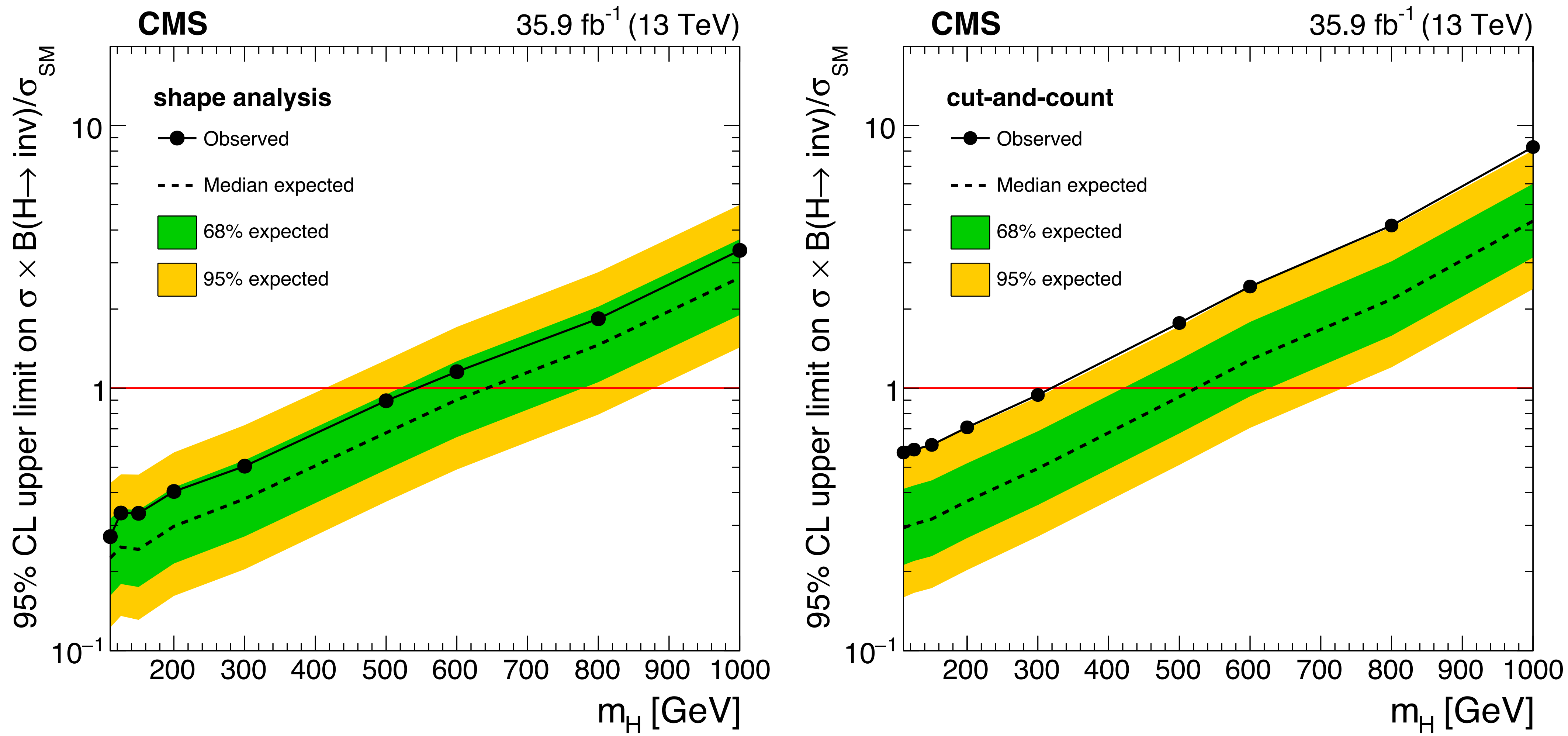

- ULs on the production cross section and branching fraction for an additional Higgs boson with SM-like couplings from shape analysis (left) and cut-and-count analysis (right)
- Mass of the additional Higgs boson up to ~540GeV is excluded from the shape analysis

H→Invisible in VBF

- Another approach to BR(H→inv)
- Observed ULs at 95% CL on BR(H→inv) are set as a function of the coupling modifiers k_V and k_F
- Within the 95% CL region of the LHC best fit on k_V and k_F, the obs. (exp.) UL on BR(H→inv) varies between 0.14 (0.11) and 0.24 (0.19)

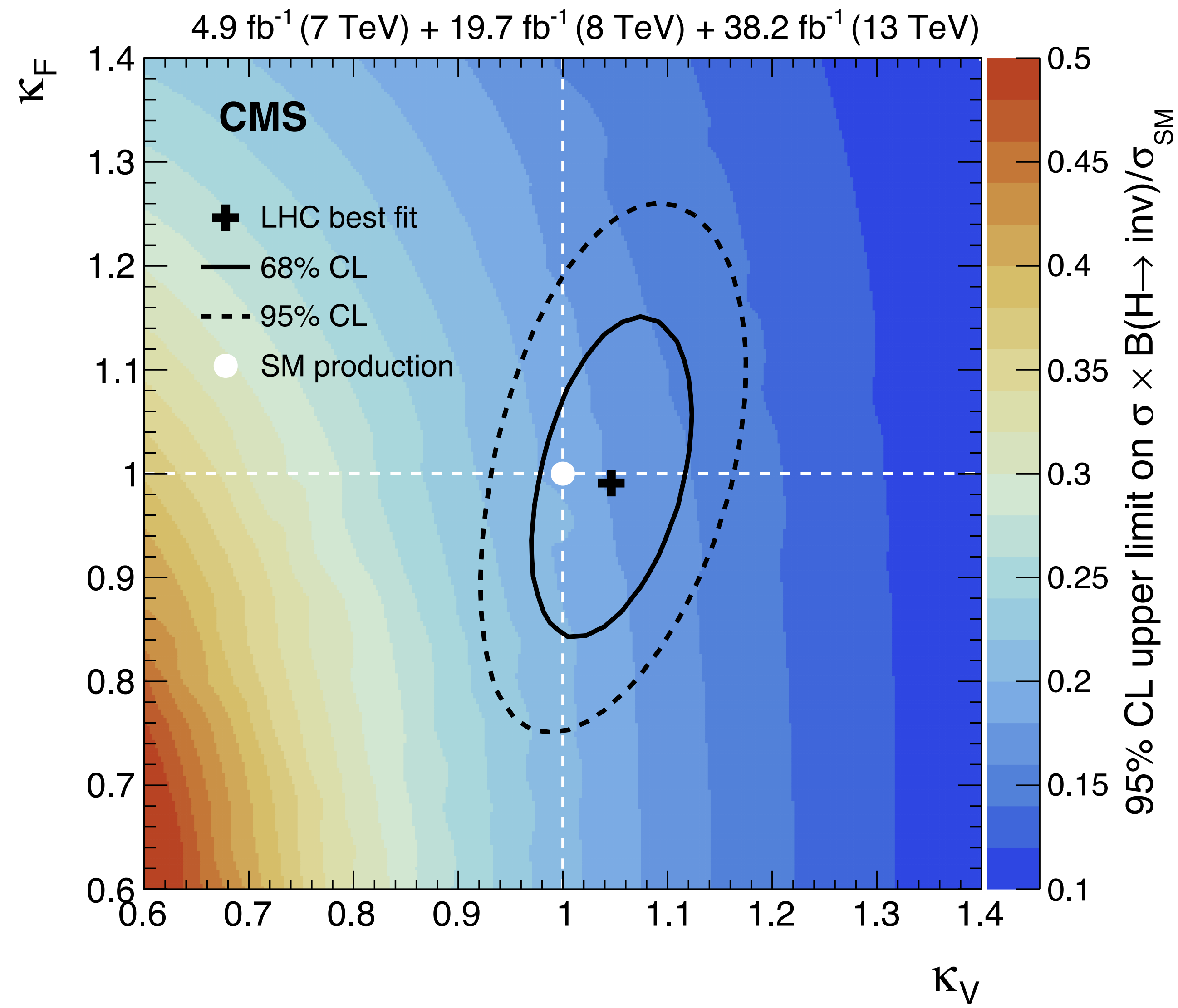

H→Invisible in Z(→ll)H

- Two well-identified leptons with $|m_{ll}-m_Z|$ <15GeV and p_T^{miss} >100GeV
- Multivariate analysis is exploited for the interpretation of the SM Higgs boson, leading to **an obs.(exp.) UL on BR(H→inv) of 0.40 (0.42)**
- Results are also interpreted in terms of Higgs portal model, Arkani-Hame-Dimopoulos-Dvali (ADD) model with large extra spatial dimensions, and unparticle scenario

✦ Published at EPJC 78 (2018) 291

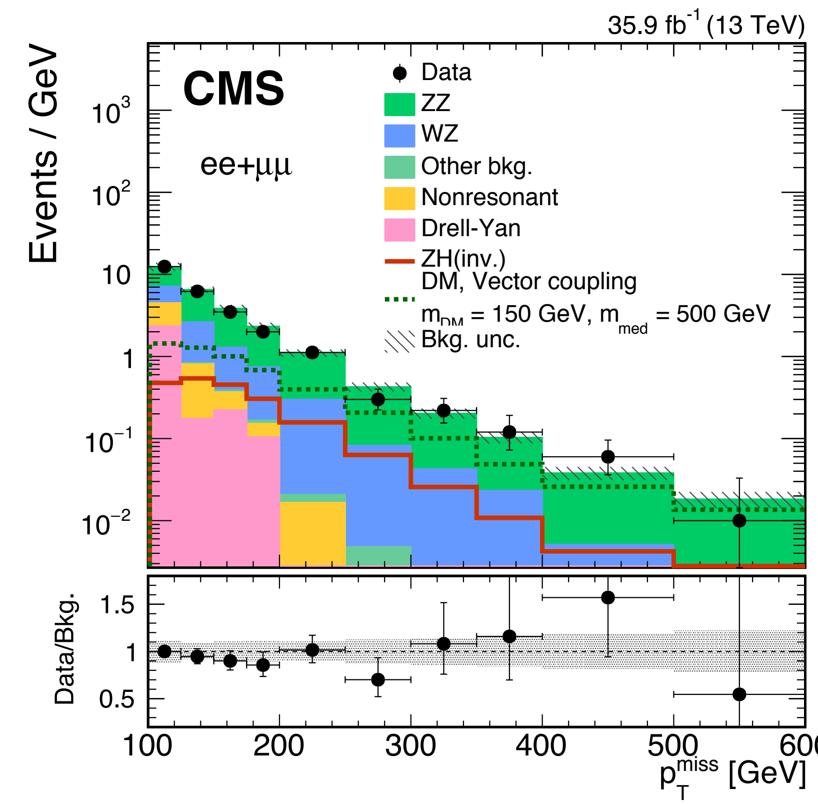

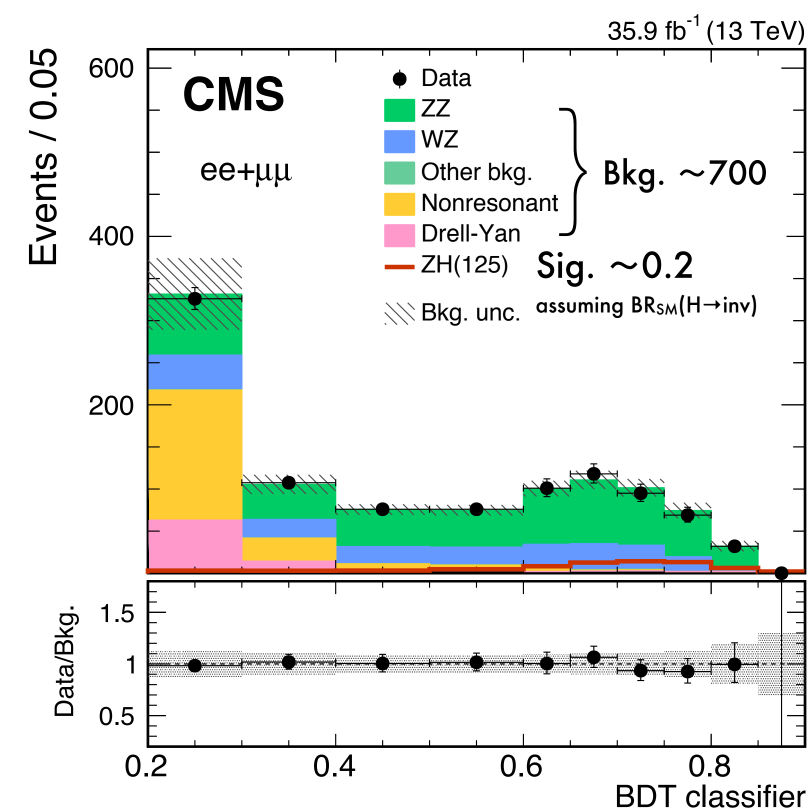

H→Invisible in V(→qq)H — mono-V

- An AK8 jet with substructure compatible with hadronic decay of Lorentz-boost W/Z boson with p_T>250GeV and |η|<2.4; p_T^{miss} >250GeV

- Larger expected signal (larger BR of V for hadronic decay than leptonic decay), but much larger background (> 3 order of magnitude than in Z(→ll)H channel)

- p_T^{miss}-based analysis, leading to **an obs. (exp.) UL on BR(H→inv) of 0.49 (0.45)**

✦ Published at PRD 97 (2018) 092005

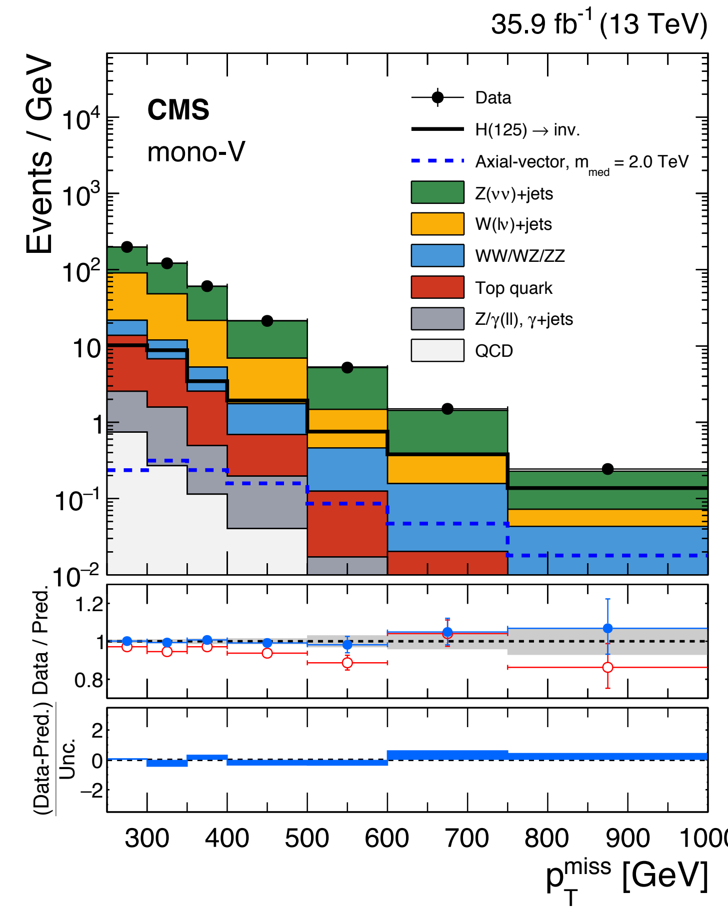

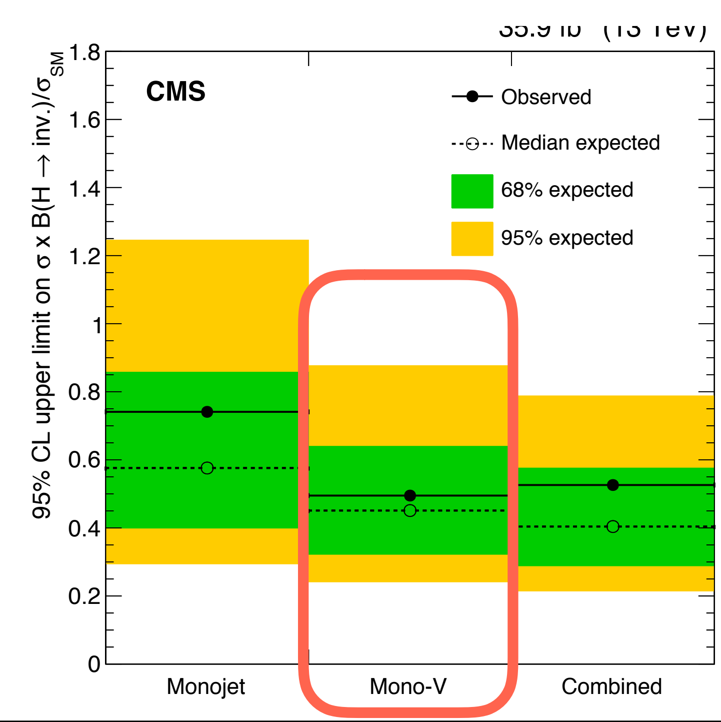

H→Invisible in ggH – monojet

- An AK4 jet with p_T>100GeV and |η|<2.4; p_T^{miss} >250GeV. Events not satisfying mono-V selection (but still passing monojet requirement) are assigned to the monojet category
- Much larger background than Z(→ll)H and mono-V category (> 2 order of magnitude than mono-V)
- p_T^{miss}-based analysis, leading to **an obs. (exp.) UL on BR(H→inv) of 0.74 (0.57)**

✦ Published at PRD 97 (2018) 092005

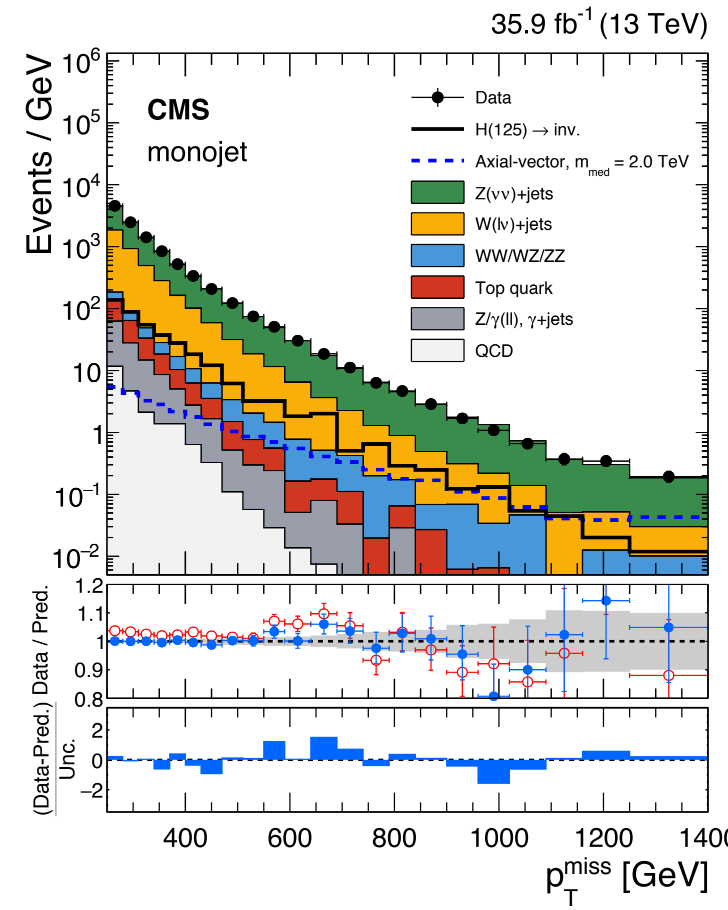

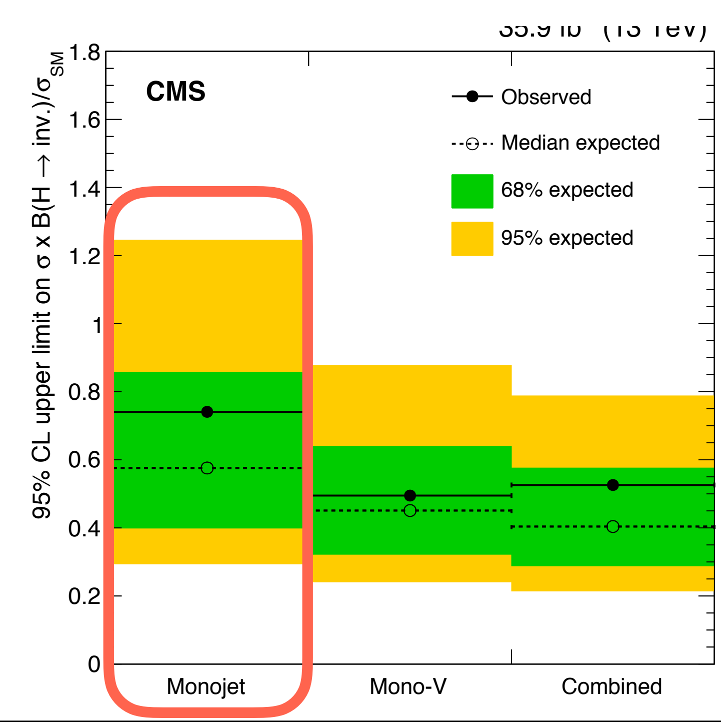

H→Invisible in V(→qq)H&ggH

Expected signal composition ggH WH ZH VBF ggZH

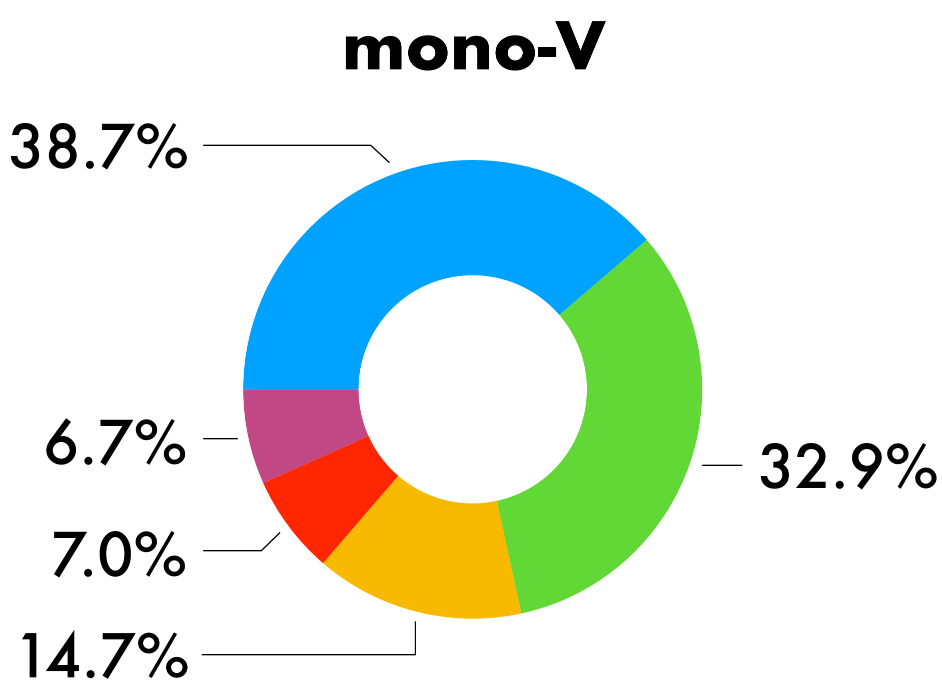

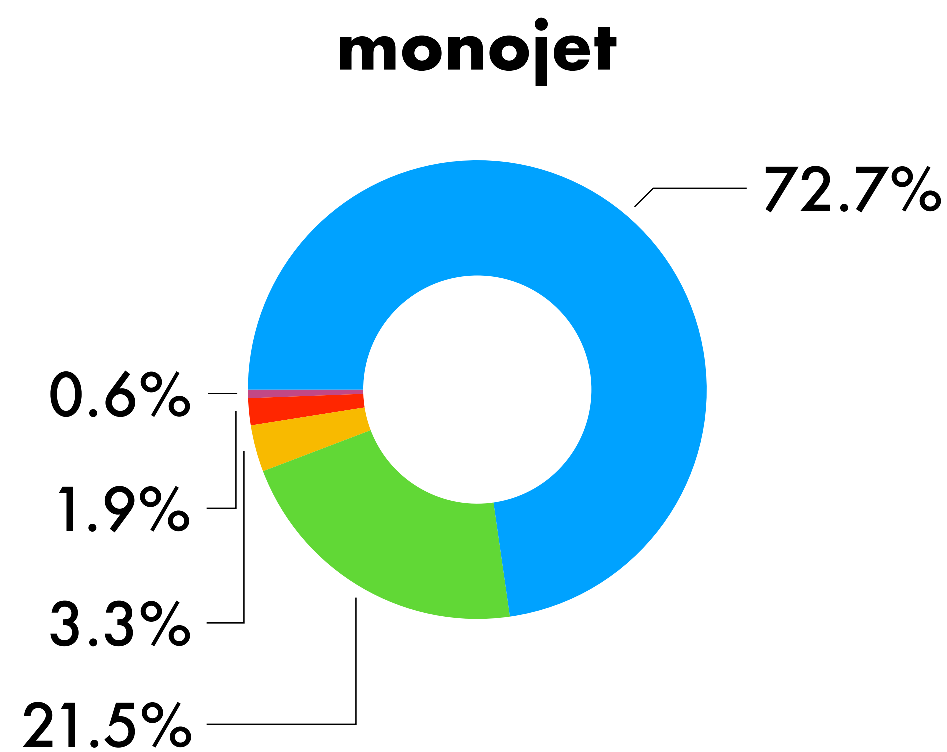

Category	Obs. (exp.) UL on BR(H→inv)
Monojet	0.74 (0.57)
Mono-V	0.49 (0.45)
Combinatio	0.53 (0.40)

- Results are also interpreted in terms of dark matter production via different mediators, fermion portal, nonthermal dark matter, and ADD model with large extra spatial dimensions

H→μμ

- The final event categories, each of whose information is shown in the table

BDT response quantile [%]	Maximum muon $\lvert\eta\rvert$	ggH [%]	VBF [%]	WH [%]	ZH [%]	$t\bar{t}H$ [%]	Signal	Bkg/GeV @125 GeV	FWHM [GeV]	Bkg fit function	$S/\sqrt{B}$ @ FWHM
0 – 8	$\lvert\eta\rvert < 2.4$	4.9	1.3	3.3	6.3	32	21.2	3.13×10^3	4.2	mBW $B_{\mathrm{deg}\,4}$	0.12
8 – 39	$1.9 < \lvert\eta\rvert < 2.4$	5.6	1.7	3.9	3.5	1.3	22.3	1.34×10^3	7.2	mBW $B_{\mathrm{deg}\,4}$	0.16
8 – 39	$0.9 < \lvert\eta\rvert < 1.9$	10	2.8	6.5	6.4	5.2	41.1	2.24×10^3	4.1	mBW $B_{\mathrm{deg}\,4}$	0.29
8 – 39	$\lvert\eta\rvert < 0.9$	3.2	0.8	1.9	2.1	3.5	12.7	7.83×10^2	2.9	mBW $B_{\mathrm{deg}\,4}$	0.18
39 – 61	$1.9 < \lvert\eta\rvert < 2.4$	2.9	1.7	2.7	2.7	0.3	11.8	4.37×10^2	7.0	mBW $B_{\mathrm{deg}\,4}$	0.14
39 – 61	$0.9 < \lvert\eta\rvert < 1.9$	7.2	3.3	6.1	5.2	1.3	29.2	9.70×10^2	4.0	mBW $B_{\mathrm{deg}\,4}$	0.31
39 – 61	$\lvert\eta\rvert < 0.9$	3.6	1.1	2.6	2.2	0.9	14.5	4.81×10^2	2.8	mBW	0.26
61 – 76	$1.9 < \lvert\eta\rvert < 2.4$	1.2	1.5	1.8	1.7	0.2	5.2	1.48×10^2	7.6	mBW $B_{\mathrm{deg}\,4}$	0.11
61 – 76	$0.9 < \lvert\eta\rvert < 1.9$	4.8	3.6	4.5	4.4	0.7	20.3	5.12×10^2	4.2	mBW $B_{\mathrm{deg}\,4}$	0.29
61 – 76	$\lvert\eta\rvert < 0.9$	3.2	1.6	2.3	2.1	0.6	13.1	3.22×10^2	3.0	mBW	0.28
76 – 91	$1.9 < \lvert\eta\rvert < 2.4$	1.2	3.1	2.2	2.1	0.2	5.8	1.04×10^2	7.1	mBW $B_{\mathrm{deg}\,4}$	0.14
76 – 91	$0.9 < \lvert\eta\rvert < 1.9$	4.4	8.7	6.2	6.0	1.1	20.3	3.60×10^2	4.2	mBW $B_{\mathrm{deg}\,4}$	0.35
76 – 91	$\lvert\eta\rvert < 0.9$	3.1	4.0	3.8	3.6	0.9	13.7	2.36×10^2	3.2	mBW	0.34
91 – 95	$\lvert\eta\rvert < 2.4$	1.7	6.4	2.5	2.6	0.5	8.6	96.0	4.0	mBW	0.28
95 – 100	$\lvert\eta\rvert < 2.4$	2.0	19	1.5	1.4	0.7	13.7	83.4	4.1	mBW	0.48
0 – 100	$\lvert\eta\rvert < 2.4$	59	61	51	52	49	253	1.30×10^4	3.9		

H→μμ

- The transformed BDT score distribution in data and simulation
- The output of the classifier was transformed such that the sum of all signal events has a uniform distribution.
- The VBF signal, corresponding to corresponds to events with the highest BDT score, can be distinguished from background processes and

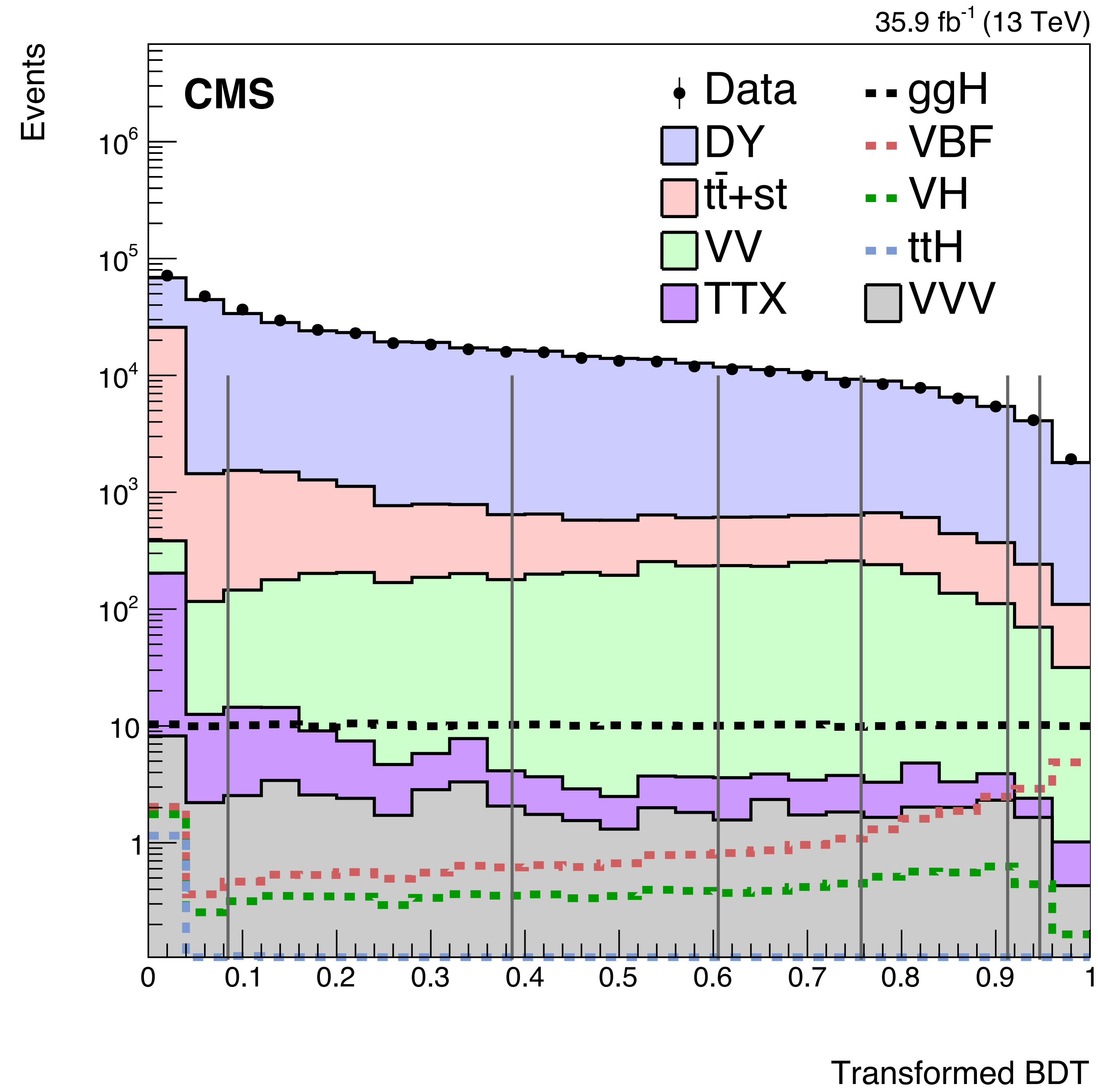

H→μμ

- Systematic uncertainties

Experimental sources	Uncertainty (%)	Type
Jet energy scale & resolution	6.0	Migrations between categories
Muon momentum scale	0.05	Modeling of the signal shape
Muon momentum resolution	10.0	
Luminosity	2.5	Expected signal yield
Lepton efficiency	2.0	
Pileup	1.0	
b-tagging & jet mistagging efficiency	1.0	Migrations between categories
Theoretical sources		
Factorization & renormalization scales	6.0	Migrations between categories
PDF choice	2.0	
Factorization & renormalization scales	0.4～10.0	Signal cross-section
PDF choice	1.6～3.7	
Branching fraction	1.7	

H→Z/γ*γ→llγ

- Leading order Feynman diagrams for H→Z/γ*γ→llγ

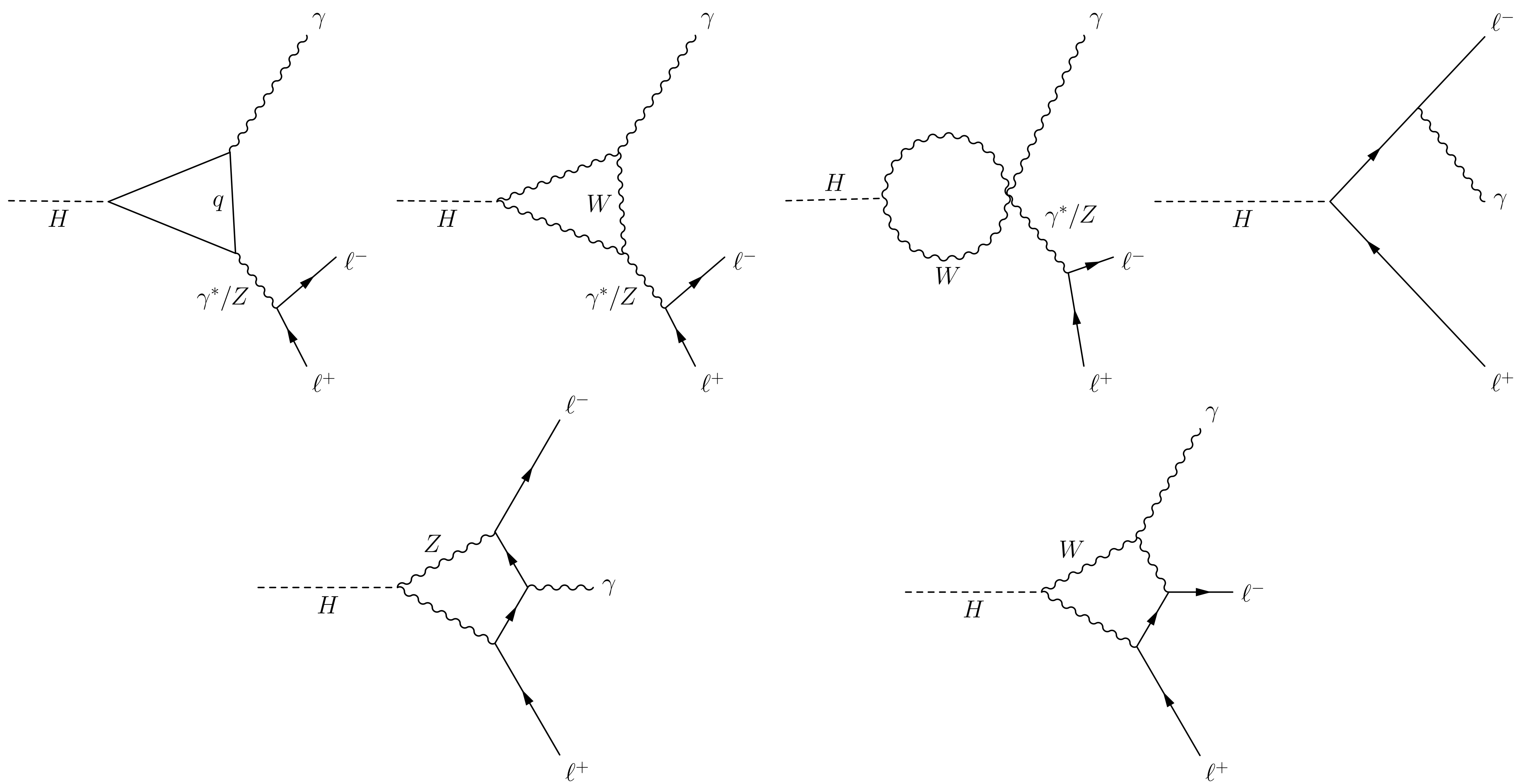

$H \to Z/\gamma^*\gamma \to ll\gamma$

- The final event categories and corresponding signal expectation

Analysis	Channel	Category	Number of signal events for $m_H = 125\,GeV$ ggH	VBF	$VH + t\bar{t}H$
$H \to \gamma^*\gamma \to \mu\mu\gamma$	$\mu\mu$	EB, high R_9	9.18	0.47	0.33
	$\mu\mu$	EB, low R_9	5.17	0.27	0.18
	$\mu\mu$	EE	3.80	0.20	0.25
	$\mu\mu$	Dijet tag	0.45	0.39	0.01
$H \to Z\gamma \to \ell\ell\gamma$	$ee + \mu\mu$	Lepton tag	0.08	0.014	0.33
	ee	Dijet tag	0.34	0.47	0.02
	ee	Boosted	3.38	0.56	0.33
	ee	Untagged 1	5.2	0.15	0.06
	ee	Untagged 2	3.2	0.09	0.04
	ee	Untagged 3	3.9	0.12	0.06
	ee	Untagged 4	2.8	0.08	0.04
	$\mu\mu$	Dijet tag	0.44	0.62	0.02
	$\mu\mu$	Boosted	4.51	0.74	0.44
	$\mu\mu$	Untagged 1	7.6	0.22	0.097
	$\mu\mu$	Untagged 2	4.8	0.14	0.06
	$\mu\mu$	Untagged 3	4.1	0.12	0.06
	$\mu\mu$	Untagged 4	3.5	0.11	0.06

H→Z/γ*+γ→llγ

- Systematic uncertainties

Sources	$H \to Z\gamma \to \ell\ell\gamma$	$H \to \gamma^*\gamma \to \mu\mu\gamma$
Theory		
– ggH cross section (scale)	3.9%	3.9%
– ggH cross section (PDF)	3.2%	3.2%
– VBF cross section (scale)	+0.4% − 0.3%	+0.4% − 0.3%
– VBF cross section (PDF)	2.1%	2.1%
– WH cross section (scale)	+0.5% − 0.7%	+0.5% − 0.7%
– WH cross section (PDF)	1.9%	1.9%
– ZH cross section (scale)	+3.8% − 3.1%	+3.8% − 3.1%
– ZH cross section (PDF)	1.6%	1.6%
– $t\bar{t}H$ cross section (scale)	+5.8% − 9.2%	—
– $t\bar{t}H$ cross section (PDF)	3.6%	—
Underlying event and parton shower		
– Muon channel	3%	4.7%
– Electron channel	3%	—
Branching fraction	5.7%	6%
Integrated luminosity	2.5%	2.5%
Lepton identification and isolation		
– Muon channel	0.6%	2%
– Electron channel	1.2%	—
Photon identification and isolation		
– Muon channel	2.3%	1.6%
– Electron channel	2.2%	—
Pileup reweighting		
– Muon channel	0.6%	0.3%
– Electron channel	0.9%	—
R_9 reweighting		
– Muon channel	6.5%	9%
– Electron channel	6.8%	—
Trigger		
– Muon channel	1.3%	4%
– Electron channel	1%	—
Energy and momentum (muon channel)		
– Signal mean	0.04%	0.08%
– Signal resolution	4%	5%
Energy (electron channel)		
– Signal mean	0.15%	—
– Signal resolution	4%	—
Jet energy scale		
– Muon channel	2.5%	3.8%
– Electron channel	2.7%	—
Jet energy resolution		
– Muon channel	0.3%	0.7%
– Electron channel	0.3%	—

H→Z/γ*γ→llγ

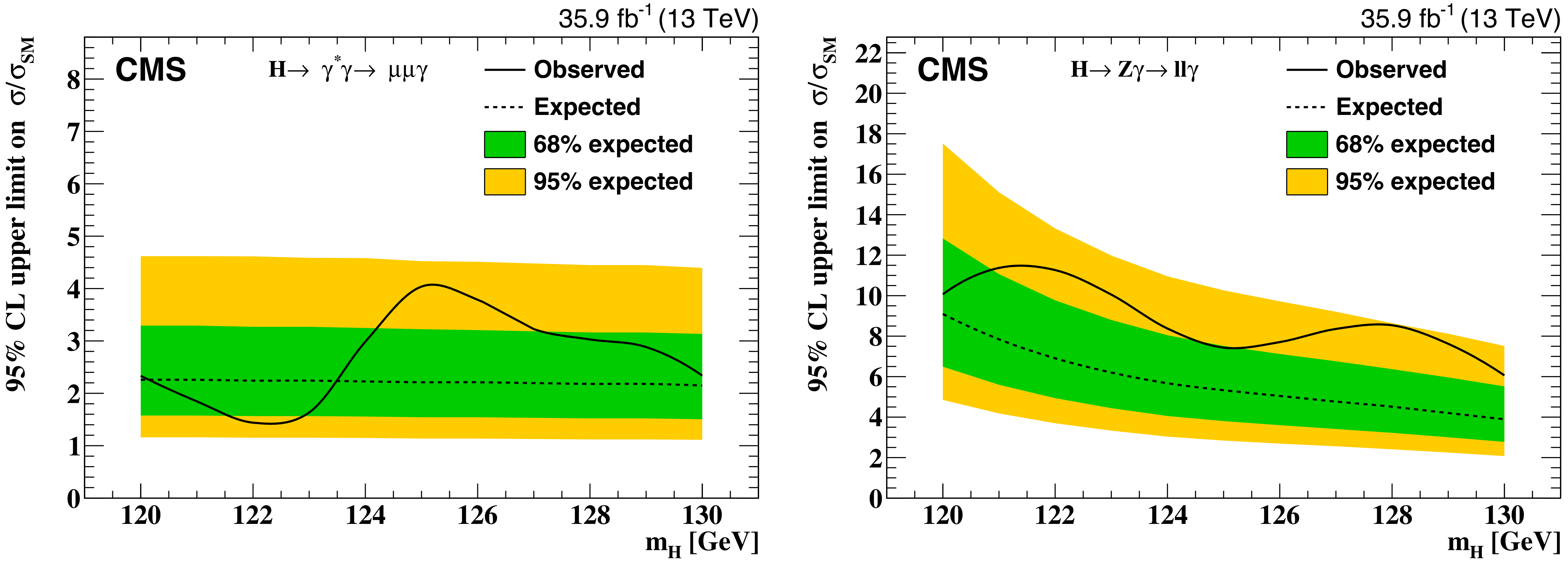

- ULs on signal strength σ/σ_{SM} are calculated in $120<m_H<130$ GeV
- H→γ*γ: 1.4~4.0 (2.1~2.3)×SM prediction; H→Zγ: 6.1~11.4 (3.9~9.1)×SM prediction for abs. (exp.) ULs
- H→γ*γ channel has comparable sensitivity with H→μμ channel

H/Z→J/ψ γ→μμγ

- Leading order Feynman diagrams for H/Z→J/ψ γ→μμγ

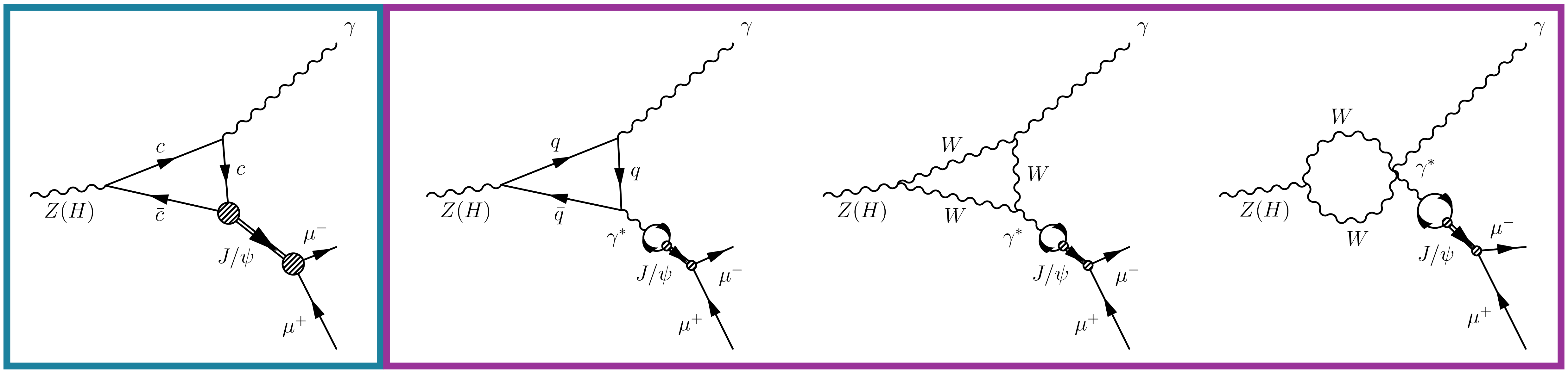

Direct process **Indirect processes**

- Considering only direct process leads to a BR of O(∼10^{-8})
- Considering only indirect process(es) leads to a BR of O(≳10^{-6})
- Considering all processes with the interference being properly taken into account leads to a BR of 3.0×10^{-6}

H→$c\bar{c}$ in BSM

- In some extensions to the SM, modified H$c\bar{c}$ coupling can arise
  - In the context of the effective field theory, H$c\bar{c}$ coupling is modified in the presence of dimension-six operator
    - An enhancement may occur at the cutoff scale Λ
  - Two-Higgs-Doublet model with minimal flavor violation
    - The coupling can be constructed in such a way that H$c\bar{c}$ is enhanced with other couplings not severely affected
  - The composite pseudo-Nambu-Goldstone boson model
    - Can be constrained by the direct search for the composite particles associated with the charm quark

Ref: PRD. 89, 033014

BR($H \to J/\psi\ \gamma$) v.s κ_c

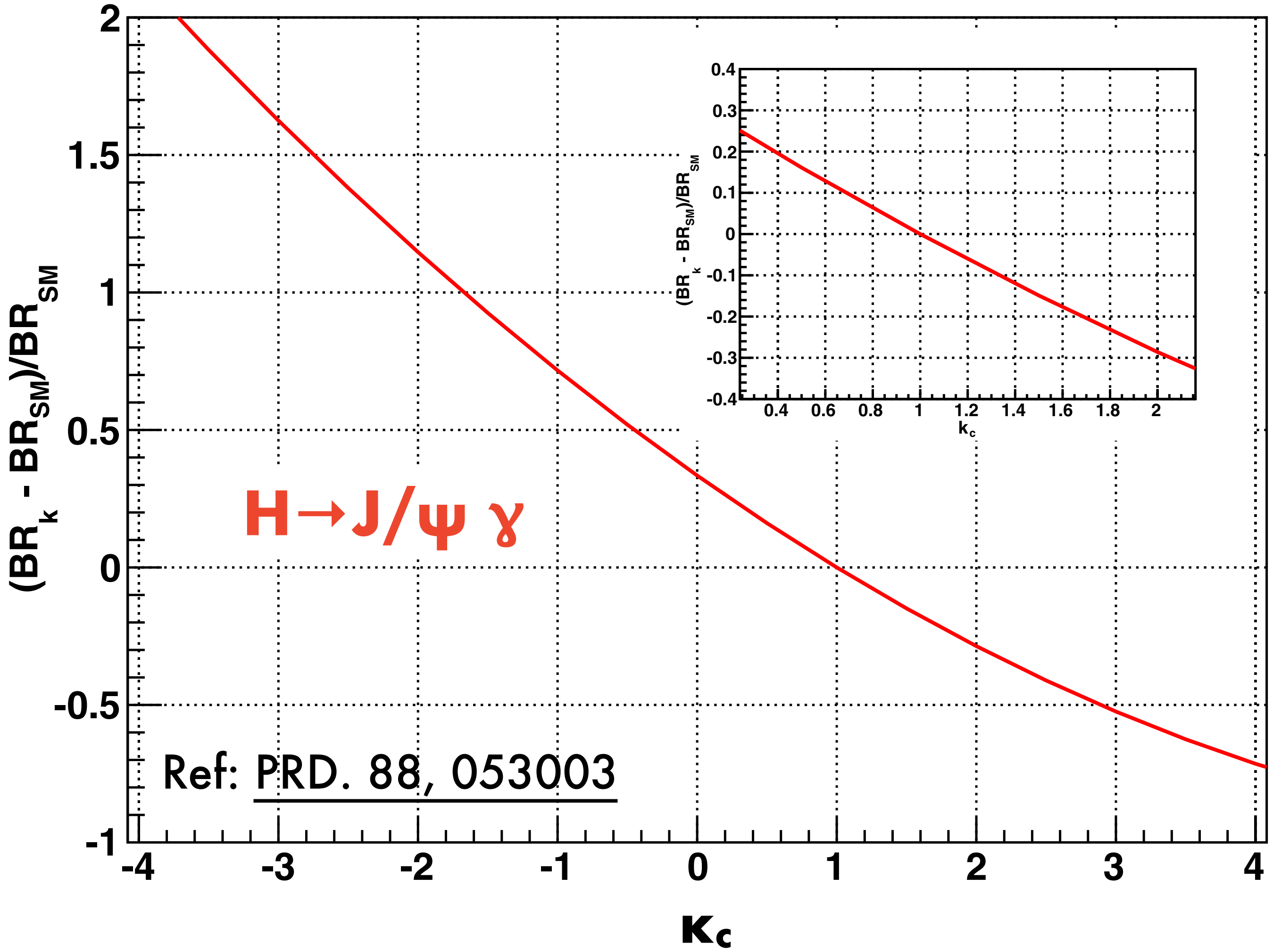

- Deviation from SM prediction for the couplings affects the interference terms and results in changes in the branching fraction
  - $Hc\bar{c}$ coupling deviates 2 times from its SM value ➜ a shift in the branching fraction > 100%
- The interference can tell us more information
  - Which sign does κ_c have, relative to other coupling constants?

$H/Z \to J/\psi\, \gamma \to \mu\mu\gamma$

- Resonant background - those will exhibit a peak in $m_{\mu\mu\gamma}$ spectrum
  - For $Z \to J/\psi\, \gamma$ decay : $Z \to \mu\mu\gamma_{FSR}$ process
  - For $H \to J/\psi\, \gamma$ decay :
    - $H \to \gamma^*\gamma$ (Higgs Dalitz decay)
    - $H \to \mu\mu + \gamma_{FSR}$: a photon radiated from one of the muons. After the event selection, the contribution of this background is found to be negligible
- The resonant backgrounds are subtracted when deriving the limits

H/Z→J/ψ γ→μμγ

Process	Description
Inclusive Quarkonium + jets/γ	Muons come from the J/ψ, jet is misidentified as a photon
pp→Z/γ*(→μμ)+jets	A jet is misidentified as an energetic photon in the event
pp→γ + jets	The muons can come from the jets.

- These are background processes that do not give resonant peaks in the $m_{\mu\mu\gamma}$ spectrum
- No proper simulation samples yet available
- Modeled using the parametrized fits to $m_{\mu\mu\gamma}$ distributions in data

$H/Z \to J/\psi\ \gamma \to \mu\mu\gamma$

$Z \to J/\psi\gamma$ ($81 < m_{\mu\mu\gamma} < 101$ GeV)

Category	Signal	Obs. (exp.) non-resonant bkg.	Exp. resonant bkg.
EB high R9	0.69	69 (66.9±4.9)	2.1
EB low R9	0.42	67 (62.6±4.6)	1.2
EE	0.30	47 (43.0±4.0)	1.0

$H \to J/\psi\gamma$ ($120 < m_{\mu\mu\gamma} < 130$ GeV)

Category	Signal	Obs. (exp.) non-resonant bkg.	Exp. resonant bkg.
Inclusive	0.076	56 (51.0±3.4)	0.20

- The total signal efficiencies for the $J/\psi\ \gamma \to \mu\mu\gamma$ final states are 22 and 14 % for the Higgs and Z boson decay, respectively
- The total signal efficiency for the Z boson decay is 13% if the J/ψ meson is fully transversely polarized and 16% if it is fully longitudinally polarized.

H/Z→J/ψ γ→μμγ

Channel	Polarization	σ (fb) at 95% CL	$\mathcal{B}(\mathrm{Z\ (H)} \to \mathrm{J}/\psi\gamma)$ at 95% CL	$\frac{\mathcal{B}(\mathrm{Z\ (H)}\to \mathrm{J}/\psi\gamma)}{\mathcal{B}_{\mathrm{SM}}(\mathrm{Z\ (H)}\to \mathrm{J}/\psi\gamma)}$
	Unpolarized	$4.6\ (5.3^{+2.3}_{-1.6})$	$1.4\ (1.6^{+0.7}_{-0.5}) \times 10^{-6}$	15 (18)
$\mathrm{Z} \to \mathrm{J}/\psi\gamma$	Transverse	$5.0\ (5.9^{+2.5}_{-1.7})$	$1.5\ (1.7^{+0.7}_{-0.5}) \times 10^{-6}$	16 (19)
	Longitudinal	$3.9\ (4.6^{+2.0}_{-1.4})$	$1.2\ (1.4^{+0.6}_{-0.4}) \times 10^{-6}$	13 (15)
$\mathrm{H} \to \mathrm{J}/\psi\gamma$	Transverse	$2.5\ (1.7^{+0.8}_{-0.5})$	$7.6\ (5.2^{+2.4}_{-1.6}) \times 10^{-4}$	260 (170)

- The J/ψ meson from Z boson decay can be transversely (λ_θ = +1) or longitudinally (λ_θ = -1) polarized in the helicity frame, depending on the polarization of the Z boson
  - Would be interesting to constrain it using Z boson polarization measurements (for example, arXiv:1504.03512 and arXiv:1606.00689)

H/Z→J/ψ γ→μμγ

- Systematic uncertainties

Source	$Z \to J/\psi\gamma$ channel Signal	$Z \to J/\psi\gamma$ channel Resonant background	$H \to J/\psi\gamma$ channel Signal	$H \to J/\psi\gamma$ channel Resonant background
Integrated luminosity	2.5%			
Theoretical uncertainties				
Signal cross section (scale)	3.5%	5.0%	+4.6% -6.7%	
Signal cross section (PDF)	1.7%	5.0%	3.2%	
Branching fraction	—	5.0%	—	6.0%
Detector simulation, reconstruction				
Pileup weight	0.8%	1.8%	0.7%	1.6%
Trigger	4.0%	4.0%	3.9%	4.0%
Muon ident./Isolation	3.0%	3.4%	2.0%	2.5%
Photon identification	1.1%	1.1%	1.2%	1.2%
Electron veto	1.1%	1.1%	1.0%	1.0%
Signal model				
$m_{\mu\mu\gamma}$ scale	0.06%	—	0.1%	—
$m_{\mu\mu\gamma}$ resolution	1.0%	—	4.8%	—

$H \to QQ \to 4\mu$

- Systematic uncertainties

Experimental sources	Uncertainty
Luminosity	The impact on the upper limits < 2%
Trigger, reconstruction, identification efficiency	
Muon momentum scale and resolution	
Four-muon vertex fit	
b-tagging & jet mistagging efficiency	
Theoretical sources	
Factorization & renormalization scales	
PDF choice	
Branching fraction	

CMS v.s ATLAS

Channel	Expected limit at 95% confidence level	Reference
$H \rightarrow$ invisible	• ATLAS: BR < 0.17 • CMS: BR < 0.15 (Both performed combinations with other production modes and Run1 results)	• ATLAS: arXiv:1904.05105 • CMS: arXiv:1809.05937
$H \rightarrow \mu\mu$	• ATLAS: 2.9×SM prediction • CMS: 2.2×SM prediction (Both performed combinations with Run1 results)	• ATLAS: PRL 119 051802 • CMS: PRL 122 021801
$H \rightarrow Z\gamma$	• ATLAS: 4.4×SM prediction • CMS: 5.5×SM prediction	• ATLAS: JHEP 10 (2017) 112 • CMS: JHEP 11 (2018) 152
$H \rightarrow J/\psi\gamma$	• ATLAS: BR < 3.5×10^{-4} • CMS: BR < 5.2×10^{-4}	• ATLAS: PLB 786 (2018) 134 • CMS: EPJC 79 (2019)94

HL-LHC Projection

Channel	Projection on significance/ expected limit for $3000fb^{-1}$	Reference
H→invisible	• ATLAS: BR(H→inv) ≲ 8% (using ZH) • CMS: BR(H→inv) ≲ 5% (using VBF)	• ATL-PHYS-PUB-2013-014 • CMS-PAS-FTR-18-016
H→μμ	• ATLAS: ≳ 9σ • CMS: ~5σ with ≳$1000fb^{-1}$	• ATL-PHYS-PUB-2018-006 • CMS-CR-2014-199
H→Zγ	• ATLAS: 3.9σ • CMS: ~4σ	• ATL-PHYS-PUB-2014-006 • CMS: preliminary&private estimation
H→J/ψγ	• ATLAS: ~15×SM prediction • CMS: ≲ 20×SM prediction	• ATL-PHYS-PUB-2015-043 • CMS: preliminary&private estimation